REPUBLIC OF TÜRKİYE
AYDIN ADNAN MENDERES UNIVERSITY
GRADUATE SCHOOL OF NATURAL AND APPLIED SCIENCES
DEPARTMENT OF MECHANICAL ENGINEERING
MASTER'S PROGRAMME IN MECHANICAL ENGINEERING
2025-MSc-33

INVESTIGATION OF THE EFFECT OF CONSTRUCTIONAL PARAMETERS OF DISCRETE ATTACHMENTS ON ENERGY TRANSFER FROM A VIBRATION SOURCE

Serkan MANTAR

MASTER'S THESIS

SUPERVISOR

Assoc. Prof. Dr. Turgay ERAY

AYDIN – 2025

ACCCEPTANCE AND APPROVAL

The thesis titled ‘’INVESTIGATION OF THE EFFECT OF CONSTRUCTIONAL PARAMETERS OF DISCRETE ATTACHMENTS ON ENERGY TRANSFER FROM A VIBRATION SOURCE’’, prepared by Serkan MANTAR, a student of Department of Mechanical Engineering Program at Republic of Türkiye Aydın Adnan Menderes University, Graduate School of Natural and Applied Sciences, was accepted as a Master’s Thesis by the jury below.

Date of Thesis Defence: 25.06.2025

Jury Member

APPROVAL:

Chair (Supervisor)	: Assoc. Prof. Dr. Turgay ERAY Aydin Adnan Menderes University	.....
Member	: Dr. Mustafa TIMUR Aydin Adnan Menderes University	.....
Member	: Dr. Salih DEMIRTAS Erzincan Binali Yildirim University	.....

This thesis was approved by the jury above in accordance with the relevant articles of the Aydın Adnan Menderes University Graduate Education and Examination Regulations and was approved on the .....by from the Board of Directors of the Graduate School of Natural and Applied Sciences in the ..... numbered decision.

Prof. Dr. Ethem AKTURK

Institute Director

Dedicated to my father and my mother.

ACKNOWLEDGEMENTS

I would like to sincerely thank my advisor, Assoc. Prof. Dr. Turgay Eray, who stood by me not only as a mentor but also as a big brother throughout this journey. His endless support, encouragement and wise guidance were always a source of strength for me.

My heartfelt thanks go to my beloved parents, Hülya Mantar and Osman Mantar, who never stopped believing in me and were always by my side with their endless support love.

My sincere thanks also go to all the teachers and mentors whose names I can not possibly list one by one, but whose contributions have been deeply impactful throughout my academic and personal development.

Lastly, I dedicate this thesis to my elder brother, whose memory I cherish deeply.

Serkan MANTAR

SCIENTIFIC ETHICS STATEMENT

I hereby declare that I composed all the information in my Master's thesis entitled ''INVESTIGATION OF THE EFFECT OF CONSTRUCTIONAL PARAMETERS OF DISCRETE ATTACHMENTS ON ENERGY TRANSFER FROM A VIBRATION SOURCE'' within the framework of ethical behavior and academic rules, and that due references were provided and for all kinds of statements and information that do not belong to me in this study in accordance with the guide for writing the thesis. I declare that I accept all kinds of legal consequences in case of any contrary statement of what I have stated is revealed.

.....

Serkan MANTAR

23.07.2025

TABLE OF CONTENTS

LIST OF FIGURES

LIST OF TABLES

ÖZET

AYRIK EKLENTİLERİN KONSTRÜKTİF PARAMETRELERİNİN BİR TİTREŞİM KAYNAĞINDAN ENERJİ TRANSFERİNE ETKİSİNİN İNCELENMESİ

Mantar S., Aydın Adnan Menderes Üniversitesi, Fen Bilimleri Enstitüsü, Makine Mühendisliği Anabilim Dalı, Yüksek Lisans Tezi, Danışman: Doç. Dr. Turgay ERAY, Aydın, 2025.

Titreşim doğasında sahip olduğu yıkıcı etkilerden dolayı sistemelerde, yapılarda, makine parçalarında pek istenmez. Bu istenmeyen etki beraberinde yitip giden belirli miktarlarda enerjiyi yanında taşır. Faydasız enerjinin toplanıp daha sonra kullanılabilir mi sorusu birçok araştırmacıyı motive etmiştir. Bu çalışmada benzer düşünceyle ulaşılmak istenilen hedefin gerçekleştirilmesi adına çelik malzemeli bir plaka ana yapı olarak kullanılmıştır. Bu ana yapının üzerine plakanın hem x hem de y eksenlerinde simetrik olacak şekilde farklı adetlerde ve farklı konumlamalarda kütle ve yay elemanlarından oluşan eklentiler konmuştur. Bu eklentiler güç tüketen elektronik cihazlarda kullanılmak üzere enerji toplayıcılar olarak düşünülmüştür.

Çok sayıda elemanın birlikte olan davranışlarını incelemek amacıyla sonlu elemanlar metodu kullanılmıştır. Eklentilerin doğal frekansları ile plakanın ilk modunun frekansı denk getirilmiştir. Eklenti kütlelerinin ağırlıkları toplamının ana yapının ağırlığına oranının 1/10'dan küçük olmasına dikkat edilmiştir. Eklenti yaylarının kütleleri dikkate alınmamıştır. Plaka üzerinden eklentilere geçen kinetik enerji (kütle) ve potansiyel enerji (yay) değerlerinin bulunmasına yönelik, plaka 1 ve 2. serbest titreşim modlarında tam ortasından harmonik yerdeğiştirme olarak plaka tahrik edilmiştir.

Sonuçlardan görüldüğü üzere eklentilerin doğal frekansları ile plakanın ilk doğal frekansıyla aynı tutulmasına yönelik eklenti parametreleri değiştirildiğinde plakaya uygulanan harmonik tahriğin ilk modda yapılması durumunda en yüksek enerji elde edilmiştir. Eklenti sayısı arttıkça toplam enerjinin arttığı, fakat birim eklenti başına

enerjinin düştüğü görülmüştür. Plakanın dört kenarındaki sınır koşulları sabit (herhangibir harekete izin verilmeyecek şekilde) seçildiğinden plakanın merkezine doğru eklentiler yerleştirildiğinde enerji artışı gözlemlenmiştir. Plakayla eklentilerin denk getirilen frekansları değiştirilip eklentilerin kütleleri sabit tutulup yay rijitliği etkisine bakıldığında ve rijitlik sabit tutulup kütle etkisine bakıldığında en çok enerjinin frekans oranının 1 olduğu durum olarak bulunmuştur.

Anahtar Kelimeler: Plaka titreşimleri, Ayrık eklentiler, Enerji hasatlama

ABSTRACT

INVESTIGATION OF THE EFFECT OF CONSTRUCTIONAL PARAMETERS OF DISCRETE ATTACHMENTS ON ENERGY TRANSFER FROM A VIBRATION SOURCE

Mantar S. Aydın Adnan Menderes University, Graduate School of Natural and Applied Sciences, Department of Mechanical Engineering, Master's Thesis, Supervisor: Assoc. Prof. Dr. Turgay ERAY, Aydin, 2025.

Due to the destructive effects inherent in vibration, it is generally undesirable in systems, structures and machine components. This unwanted effect also carries with it the loss of a certain amount of energy. The question of whether this lost, useless energy can be collected and reused has motivated many researchers. Attachments composed of mass and spring elements were placed on the main structure in varying numbers and positions, symmetrically along both the x and y axes of the plate. These attachments were considered as energy harvesters to be used in power-consuming electronic devices.

The finite element method was used to investigate the coupled behavior of multiple elements. The natural frequencies of the discrete attachments were tuned to be identical with the first mode of the bare plate. It has been ensured that the total weight of the attachment masses remains less than one-tenth of the main structure's weight. The mass of the springs used in the attachments has not been taken into account. To determine the kinetic energy (mass) and potential energy (spring) transferred from the plate to the attachments, the plate has been harmonically excited at its center in the first and second free vibration modes.

As observed from the results, the highest energy has been obtained when the harmonic excitation is applied in the first mode of the plate, provided that the attachment parameters are adjusted to match the natural frequencies of the attachments with the first natural frequency of the plate. It was found that while the total harvested energy increased with the number of attachments, the energy per attachment decreased.

Since all four edges of the plate are fixed (restricting any movement), an increase in energy has been observed when the attachments are placed closer to the center of the plate. When the coupled frequencies of the bare plate and attachments were varied – first by keeping the mass constant and by changing the spring stiffness, and then by keeping the stiffness constant and changing the mass – it was determined that the highest energy was obtained when the frequency ratio was equal to 1.

Keywords: Plate vibrations, Discrete attachments, Energy harvesting

1. INTRODUCTION

This thesis investigates the effects of structural parameters of discrete attachments that were placed on the plate, such as their mass, stiffness, number, spatial arrangement, and damping properties, on energy transfer and energy harvesting. Initially, the definition of plate and its relevance to plate theories will be discussed. "*A plate is a structural element with planform dimensions that are large compared to its thickness and is subjected to loads that cause bending deformation in addition to stretching* (Reddy, 2007)."

In their book (Timoshenko & Woinowsky-Krieger, 1989), they emphasize that plates' bending characteristics depend more on their thickness than on other dimensions. They classify plates into three groups based on their thickness relative to other dimensions: thin plates with small deflections, thin plates with large deflections, and thick plates.

The development of plate theories evolved starting with Kirchhoff's classical plate theory (CPT) around 1850, which is suitable for thin plates and neglects shear effects. In 1950, Mindlin's theory also known as the first-order shear deformation theory (FSDT), was introduced for thicker plates and accounts for shear effects. By the 1980s, higher-order shear deformation plate theories (HSDT) emerged, offering improved kinematic representation, particularly for composite plates, and incorporating shear effects (Kolvik, 2012).

The application of these theories becomes crucial in real-world systems, as the vibrational plates play a significant role in the analysis of practical structures such as bridge decks, hydraulic structures, pressure vessel covers, pavements of highways and runways, ship decks, airplanes, missiles, and machine components (Rao, 2007).

After providing a general overview of plate theories and their vibrational behaviors it becomes deeper into how various attachments, such as masses and springs, influence these behaviors. Investigating the effects of these attachments aids in comprehending and predicting the dynamic responses of plates under different loading conditions.

Vibration attenuation is essential due to its potential to cause catastrophic failures in systems. This issue has long been a focus in engineering, leading to the development of various solutions aimed at reducing the dynamic responses induced by these vibrations in structures (Özgüven, 2024). A conventionally tuned vibration absorber is a single-degree-of-freedom device designed to mitigate undesirable resonances or reduce structural vibrations at a specific excitation frequency (Wagner & Helfrich , 2017). Hermann Frahm introduced the concept of the dynamic vibration absorber (DVA) over a century ago (Ahmed et al., 2020). Frahm's dynamic vibration absorber is an undamped system that effectively reduces vibrations when the excitation frequency closely matches its natural frequency. However, its performance significantly deteriorates if the excitation frequency deviates from this natural frequency (Rana & Soong, 1998). Dynamic vibration absorbers, composed of mass-spring-damper mechanisms connected to the primary structure, are commonly applied in engineering – especially in their basic linear configuration – for minimizing vibrations, and they perform particularly well under steady-state harmonic excitation (Samani et al., 2013).

In line with our study, a closer examination of undamped vibration absorbers will be conducted.

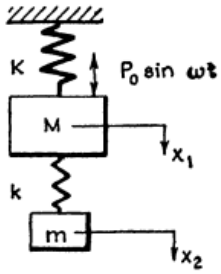

Figure 1.1. The undamped dynamic vibration absorber (Den Hartog, 1947).

In our study, similar to Den Hartog's study Figure 1.1 depicts the primary structure represented by the capital letters M and K, denoting the mass and stiffness of the plate, respectively. Additionally, the lowercase letters m and k symbolize the discrete attachments or dynamic vibration absorbers, consisting of a mass and spring.

So far, general information has been given about plate theories and dynamic vibration absorbers. The subsequent section will provide information on energy harvesting systems.

Energy harvesting can be described in its most basic form as the process of converting unused environmental energy into electrical energy, which can be either used right away or stored for future use (Toprak & Tigli, 2014).

Over the past decade, vibration-based energy harvesting has gained significant interest. This growing focus is largely driven by the decreasing power demands of small electronic devices, such as wireless sensor networks employed in passive and active monitoring systems. The primary objective in this field is to harness ambient vibrational energy to power these low-energy electronic components (Erturk & Inman, 2011).

When a device experiences vibration, an inertial mass can generate movement. This movement can then be converted into electrical energy through three methods: piezoelectric, electrostatic, and electromagnetic. The energy being harnessed in this case is mechanical energy (Chalasani & Conrad, 2008).

Piezoelectric transduction is the leading method for harvesting mechanical energy due to its superior electromechanical coupling factor and piezoelectric coefficient, especially when compared to electrostatic, electromagnetic, and triboelectric transductions (Sezer & Koç, 2021).

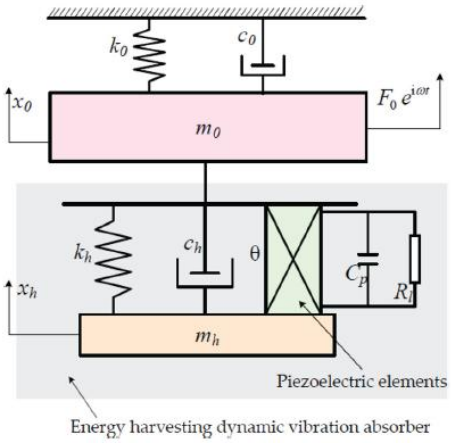

Figure 1.2. Schematic diagram of coupled system (Ali & Adhikari, 2013).

As in Figure 1.2, the main structure and the dynamic vibration absorber should be combined to form a unified structure for energy harvesting.

2. LITERATURE REVIEW

Beams and plates are fundamental components in the design of mechanical, electromechanical, and civil systems. Since many of these systems experience dynamic loading, the natural frequencies and mode shapes of linear elastic beams – featuring various configurations, boundary conditions, and attachments – have been extensively investigated over the past sixty years (Magrab, 2007). Gürgöze (1994) has derived the frequency equation of a cantilever Bernoulli–Euler beam carrying both a tip mass and a discrete spring–mass attachment using the Lagrange multiplier method, as illustrated in Figure 2.1. The study has demonstrated that the inclusion of the spring–mass system leads to a reduction in the beam's natural frequency, primarily due to the added inertia. It has also been shown that increasing the distance between the tip mass and the spring–mass attachment causes a further decrease in the natural frequency. Furthermore, the analysis has revealed that under specific configurations, the natural frequency of the system can approach zero, indicating a critical condition where the restoring force becomes insufficient to counteract the inertia of the attachments.

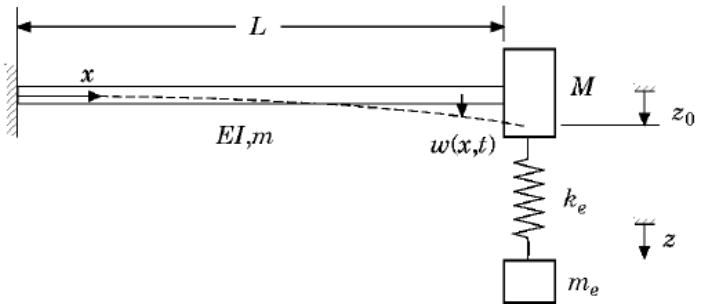

Figure 2.1. Cantilevered Bernoulli-Euler beam with a tip mass and a spring-mass system (Gürgöze, 1994).

Katı and Gökdağ (2019) have applied the semi-numerical multi-step differential transform method (MDTM) for the free vibration analysis of a beam with a tip mass, as illustrated in Figure 2.2, and have compared the results with those obtained using the commercial multiphysics software ANSYS. Parametric analyses conducted under fixed

boundary conditions have shown that the natural frequencies of the system increase as the beam length decreases, which has been attributed to the enhanced stiffness of shorter beams. The results obtained from both MDTM and ANSYS have been found to be in good agreement.

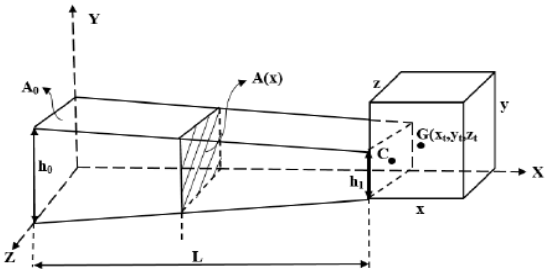

Figure 2.2. Beam-tip mass system (Katı & Gökdağ, 2019).

Wu and Chou (1998) performed a free vibration analysis of a cantilever beam carrying multiple elastically attached point masses as depicted in Figure 2.3. Their results were compared with those obtained using the finite element method. It has been found that increasing the number of attached masses leads to a noticeable decrease in the natural frequencies, primarily due to the increased inertial effect of the system. In addition, it has been shown that the stiffness of the elastic supports significantly influences the vibrational characteristics, where higher stiffness values tend to shift the system behavior toward that of rigidly attached masses. Moreover, the accuracy of the analytical model has been verified through close agreement with the results obtained via the finite element method.

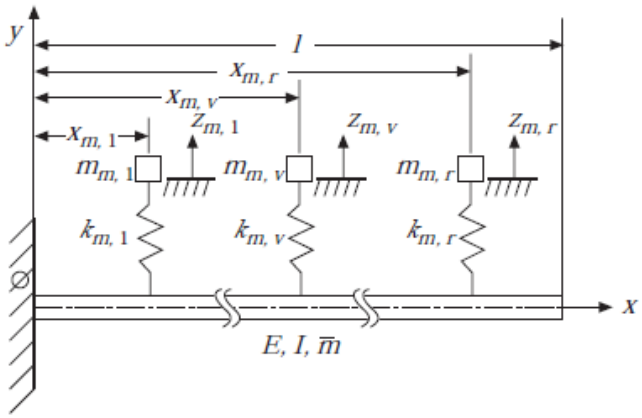

Figure 2.3. A cantilever beam carrying elastically mounted point masses (Wu & Chou, 1998).

Posiadala (1997) addressed the free transverse vibration problem of Timoshenko beams with various attachments, including translational and rotational springs, concentrated masses with moments of inertia, linear undamped oscillators, and additional supports, as modeled in Figure 2.4.

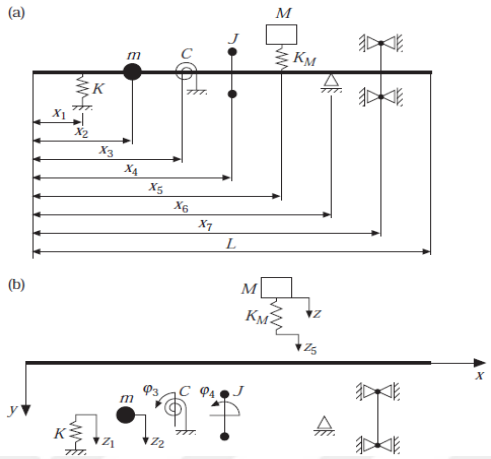

Figure 2.4. A model of the combined dynamical system (Posiadala, 1997).

Ingber et al. (1992) have investigated the vibration behavior of a clamped rectangular plate, the system with concentrated mass and spring attachments shown in Figure 2.5, using both experimental and numerical methods. Each attachment has been modeled as a lumped mass-spring unit acting as a single entity connected to the plate. Two key dimensionless parameters have been introduced: a mass parameter and a stiffness parameter. Increasing the mass parameter has reduced the natural frequencies, with the first mode becoming dominated by the motion of the attached mass. Conversely, higher the stiffness parameter highered the natural frequencies. Furthermore, the study has shown that the location of the attachment significantly affects the dynamic response of the coupled system. When the attachment is placed at or near an antinode of a mode, it induces a stronger perturbation in that mode's frequency. This position-dependence becomes especially pronounced under high mass or high stiffness conditions, where the attachment behaves like a rigid internal support.

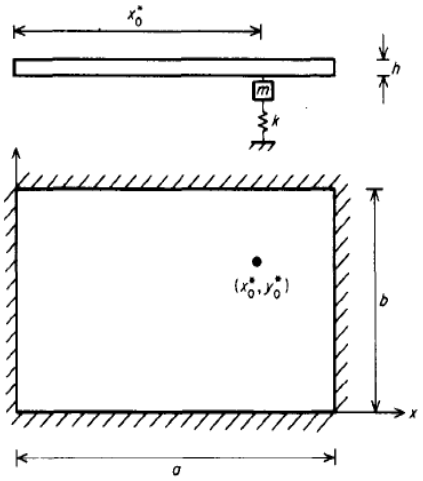

Figure 2.5. The rectangular clamped plate with spring and mass attachment (Ingber et al., 1992).

Cho et al. (2017) have investigated the vibrational behavior of rectangular plates with various discrete attachments. It has been shown that both the number and location of the attachments significantly affect the coupled system's dynamic response. Specifically, an increase in the number of attachments has generally resulted in a reduction in the natural frequencies of the coupled system, as the added masses have increased the overall inertia of the system. The attachment locations have been played a critical role. Their influence on vibrational modes and frequency shifts has become more pronounced when the locations of attachments are selected as near the high modal displacement.

Chiba and Sugimoto (2003) have investigated the vibrational behavior of a cantilever plate with an attached spring-mass system, focusing on the effects of mass ratio, stiffness ratio, and attachment location. They have found that the attachment location plays a critical role in shaping the system's dynamic response. An increase in the mass ratio (defined as the ratio of the attached mass to the plate mass) has caused a noticeable reduction in natural frequency, while a higher stiffness ratio (defined as the ratio of attachment stiffness to the plate stiffness) has resulted in behavior resembling that of a rigidly attached mass.

Yu (2009) has conducted a comprehensive analytical investigation on the free and flexural vibrations of cantilever plates carrying a single concentrated mass. The effects of mass ratio (defined as the ratio of the attached mass to the plate mass) and attachment

location on the natural frequencies and modal participation factors have been examined. The results indicate that increasing the mass ratio or placing the attachment further from the clamped edge significantly reduces the fundamental natural frequency. Furthermore, for square plates, a specific attachment location has been shown to eliminate the participation of the second symmetric mode, depending on the mass ratio.

Pavic (2006) conducted a numerical investigation on the transmitted vibration energy, energy flow, and damping behavior in a beam-plate coupled system. The model consists of a steel beam with one free end and the other end attached to a steel plate, which is simply supported on all four edges. The analyis revealed that damping significantly influences the total energy dissipation within the system, while having a limited effect on how that energy is transmitted between the beam and the plate.

The concept of energy sinks -a collection of undamped linear oscillators attached to a primary structure- has been propesed by (Koç et al., 2005) as an alternative to conventional damping methods. The study has examined the influence of frequency distribution, mass ratio (which is kept below 10%), and the number of oscillators on the energy retained by the primary structure. It has been found that increasing the mass ratio enhances the energy absorption capability of the oscillators, although this effect saturates beyond a certain point. Similarly, increasing the number of oscillators improves energy absorption and reduces energy recurrence to the primary system, but with diminishing returns after a certain number. Additionally, the frequency distribution has been optimized to minimize recurrence, and the results have confirmed that clustering oscillator frequencies around the natural frequencies of the primary structure enhances transient energy capture.

Cao et al. (2019) have investigated the dynamic behavior of rectangular plates stiffened by elastic beams under various boundary conditions and beam configurations. In this study, the beams serve as distributed attachments, forming a coupled beam–plate system. Beam length, location, and orientation have been shown to significantly influence modal characteristics, resonance behavior, and energy transmission between the beam and plate. The impact of the beams becomes more pronounced when they intersect excitation points or align with modal antinodes. Rayleigh damping has been applied in the transient simulations, reducing peak mobility amplitudes, especially in the mid-to-high frequency range.

Zheng et al. (2024) have investigated a passive vibration suppression method using distributed nonlinear energy sink (NES) cells on a corner-point supported rectangular steel plate under vertical harmonic excitation. A single NES and multiple NES's have been compared, both with equal total mass (~4.9% of the plate mass). The multiple NES configuration has achieved superior performance, reducing strain energy by up to 80% and improving damping efficiency by over 60%. As the number of NES-cells has increased, more vibrational energy has been absorbed by the attachments, leaving less in the plate, indicating effective energy redirection. An optimal number of NES-cells (seven) has been identified, beyond which further performance gains have saturated.

3. MATERIAL AND METHOD

In this thesis, the method section consists of two phases. These are;

1. Determination of constructional and controlled parameters of the coupled system composed of the plate and the discrete attachments.
2. Transient structural simulations for kinetic and strain energy results, and modal analysis for natural frequencies of the plate with and without attachments.

3.1. Determination of the Parameters of the Coupled System Composed of the Plate and the Discrete Attachments

Kirchoof – Love plate theory is used for the determination of constructional parameters. According to the assumptions in this plate theory, the dimensions of the plate, including its width, length, and thickness have been determined for the analysis. Dimensional parameters of the plate and attachments are given in Figure 3.1 and Table 3.1. Based on these dimensions and the principles of the used plate theory, the following constructional and controlled parameters have been identified for systematic analysis.

- Constructional parameters: Number of attachments, location of attachments, mass ratio, damping ratio, frequency ratio.
- Controlled parameters: Kinetic energy of attachments, strain energy of attachments, natural frequencies plate and attachments.

3.1.1. Definition of the Constructional Parameters of the Plate and the Attachments

The models used in the analyses have been coupled with the plate and the discrete attachments placed on it. Therefore, the constructional parameters such as the number of discrete attachments, their location, mass ratios (the ratio of the attached mass to the plate

mass), and frequency ratios (the ratio of attachment stiffness to the plate stiffness), have also been interrelated.

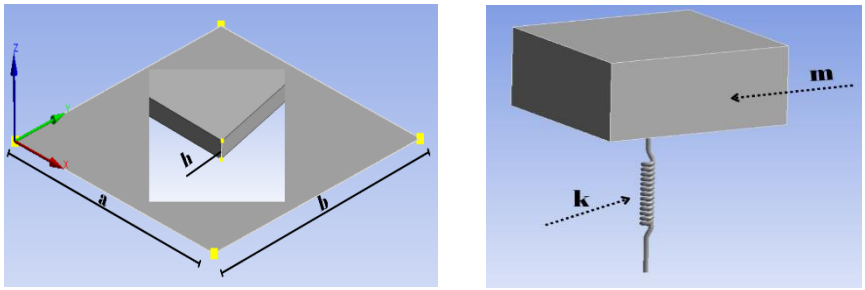

Figure 3.1. a) Dimensional representations of bare plate b) Dimensional representations of attachments.

Table 3.1. Plate and discrete attachments' dimensional parameters

	Plate	**Discrete attachments**
length(a)	1600 mm	50 mm
width(b)	1600 mm	50 mm
height(h)	2 mm	25 mm

Table 3.1 presents the dimensional properties of the plate and discrete attachments, as well as the types of materials used. In this study, the attached masses were modeled using elastic type materials such as PDMS (Polydimethylsiloxane) material. PDMS's elastic and low-density properties make it suitable for studying dynamic interaction with the host plate in vibration-based energy-harvesting systems.

Table 3.2. Constructional parameters of plate and discrete attachments

n	Number of Attachment
$[x_a, y_b]$	Location of Attachment
m	Mass of Attachment
M	Mass of Plate
m / M	Mass Ratio
k	Stiffness of Attachment
K	Stiffness of Plate
k / K	Stiffness Ratio
ω	Natural Frequency of Attachment
ώ	Natural Frequency of Plate
ω / ώ	Frequency Ratio
a	Length of Plate
b	Width of Plate
h	Thickness of Plate
b / a	Aspect Ratio

Table 3.3. Material properties of plate and discrete attachments

Material	Elastic Type	Steel Type
Mass density	**963 kg/m^3**	**7850 kg/m^3**
Elasticity modulus	**0,00147 GPa**	**210 GPa**
Poisson's ratio	**0,48**	**0,3**

Table 3.2 shows the structural parameters of the bare plate and discrete attachments. In addition, a square plate has been used by setting the aspect ratio (defined as the ratio of the plate width to the plate length) 1. It is also assumed that both the bare plate and the discrete attachments exhibit linear behavior. The discrete attachments consist of a mass and spring element. The properties of the mass element of the attachments are provided in Table 3.3. The material of the spring element of the attachments does not affect the analysis results. The coordinate system of the plate is positioned at the lower-left corner. The bare plate is clamped at all four edges. The mass elements of the attachments are considered as identical masses with the same weight. In practical applications, the total mass of the attachments is kept below 10% of the main structure's mass. In the analyses performed, it has been ensured the highest mass ratio remains below 10% based on this information.

$$\mathbf{M = \rho abh} \qquad \textbf{(3.1)}$$

The mass of the plate has been calculated using Equation (3.1) where the parameters a, b, and h are defined in Table 3.2. Mass values of the bare plate and the discrete attachments with varying number of attachments are given Table 3.4.

Table 3.4. Mass values of the plate and attachments.

Number of attachments	Total mass of the attachments(kg)	Mass of plate(kg)	Mass ratio
2	0,120376	40,192	0,002995
4	0,240752	40,192	0,005991
8	0,481504	40,192	0,011981
12	0,722256	40,192	0,017971
16	0,963008	40,192	0,023963
24	1,444512	40,192	0,035948
32	1,926016	40,192	0,04792
36	2,166768	40,192	0,05391
40	2,40752	40,192	0,0599
48	2,889024	40,192	0,07188
64	3,852032	40,192	0,09584

While investigating the mass effect, the mass values are varied. This will be discussed in the next section.

$$\omega = \sqrt{\frac{k}{m}} \qquad (3.2)$$

The frequency values of the attachments were calculated according to Equation 3.2.

3.2 Setup of the Simulations for the Modal Analysis and Transient Response

In the simulations, the plate and discrete attachments are assumed to behave linearly, and nonlinear effects are neglected. The simulations have been carried out using the ANSYS modal analysis module and transient structural module.

3.2.1 Simulation Settings Used for the Analyses in the Modal Analysis

Modal analysis of the bare plate was first performed to be used in transient analysis. The plate has a length of 1.6 meters, a width of 1.6 meters, and a thickness of 2.0 millimeters. Structural steel is assigned as the material for the plate. The plate is clamped on all four edges as boundary conditions. Figure 3.2 presents the geometric dimensions and boundary conditions of to the bare plate used in the analysis. In the analysis settings of the multiphysic simulation software (ANSYS), the maximum number of the vibrational modes is set to 6. The frequencies of the first six modes are found as follows: 6.961 Hz, 14.256 Hz, 14.256 Hz, 21.379 Hz, 25.591 Hz, and 25.788 Hz.

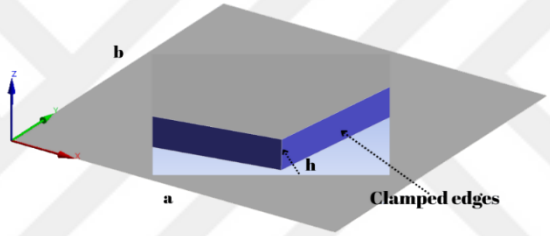

Figure 3.2. Representation of bare plate's dimensional properties and boundary condition.

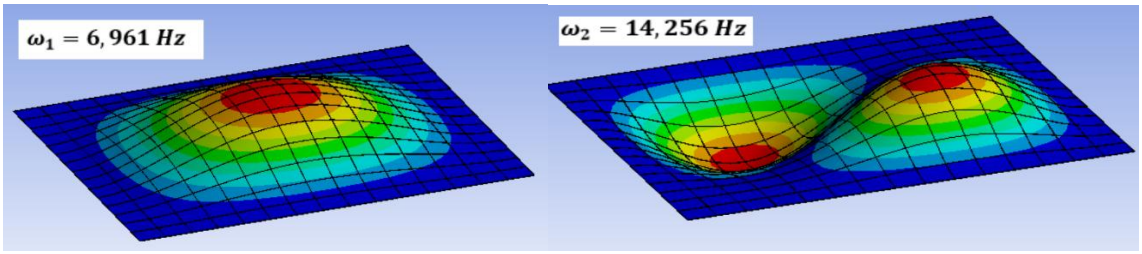

Figure 3.3. The first and second mode shapes of the bare plate.

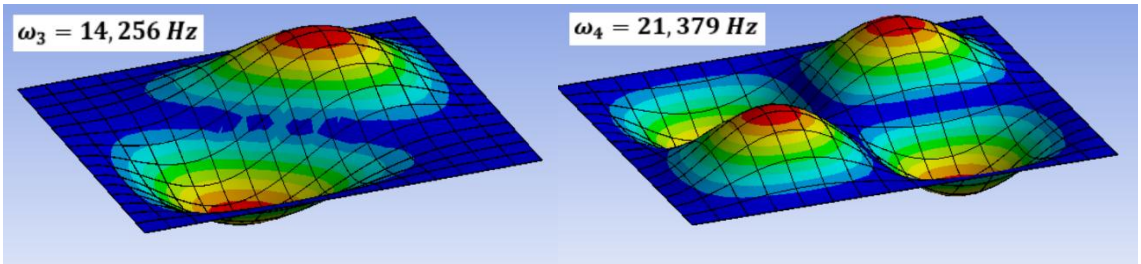

Figure 3.4. The third and fourth mode shapes of the bare plate.

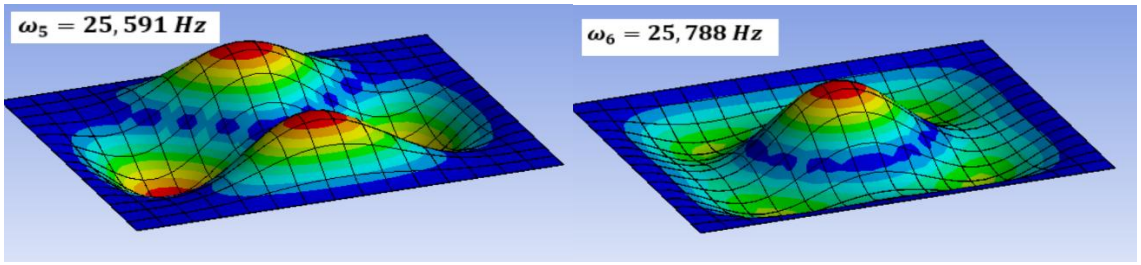

Figure 3.5. The fifth and sixth mode shapes of the bare plate.

The first and second, third and fourth, and fifth and sixth mode shapes of the bare plate are presented in Figures 3.3, 3.4, and 3.5, respectively. Each corresponding mode shapes has a particular frequency.

These results have been obtained using 1728 nodes and 225 elements, with the plate fixed all four edges.

3.2.2 Simulation Settings Used for the Analyses in the Transient Response

So far, we have obtained modal analysis results related to natural frequency. The data obtained from these modal analysis results served as our starting point for transient analyses. We ignored damping in these transient analyses. The harmonic displacement is given as yellow labels in Figure 3.6. Harmonic displacement are applied to the middle point of the bare plate. The plate was divided into as many cells as the number of attachments placed on it, and the attachments were positioned at the centers of these cells.

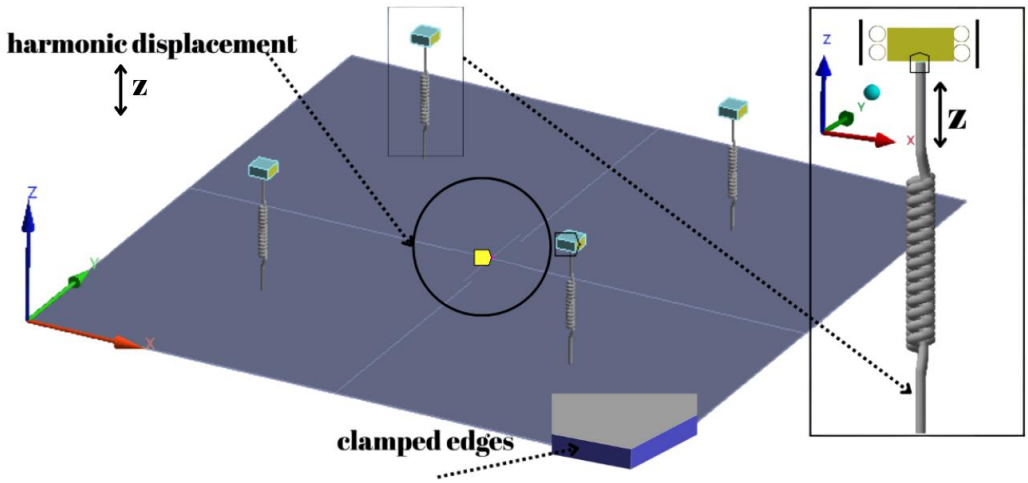

Figure 3.6. General representation of the models used in transient analyses.

In Figure 3.6, the layout and boundary conditions of four discrete attachments are given as an example. In the image given as zoom, it is shown that the attachments can only move in the z direction.

3.2.2.1 Setup Procedures for Investigating the Effect of the Number of Attachments

The plate was divided into as many cells as the number of attachments placed on it, and the attachments were positioned at the centers of these cells. The vibration input to the plate was applied as a harmonic displacement at the center point as a yellow label in Figure 3.7, with its time response given by cos(ωt) in Figure 3.8. The analyses were conducted using a mesh consisting of 4101 nodes and 546 elements. In analyses, the initial time step, minimum time step, and maximum time step were set to 0.001 seconds. With this selected minimum time step ensured that capture high mode frequency response. The attachments were allowed to be displaced only in the z direction. In this analysis set, the frequencies of the attachments were adjusted to match the first mode frequency of the bare plate. The stiffness value of the attachments was taken as k =115.2 N/m. No damping was added to the models. The frequency of the harmonic excitation $\cos(2\pi f)$ was selected as the first mode frequency of the bare plate.

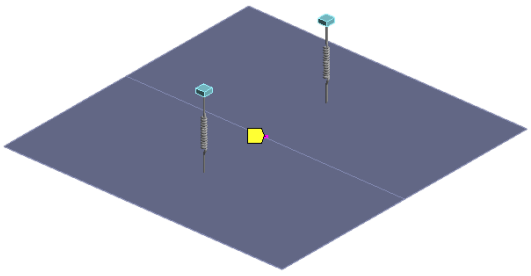

Figure 3.7. Representation of the location of the applied harmonic input

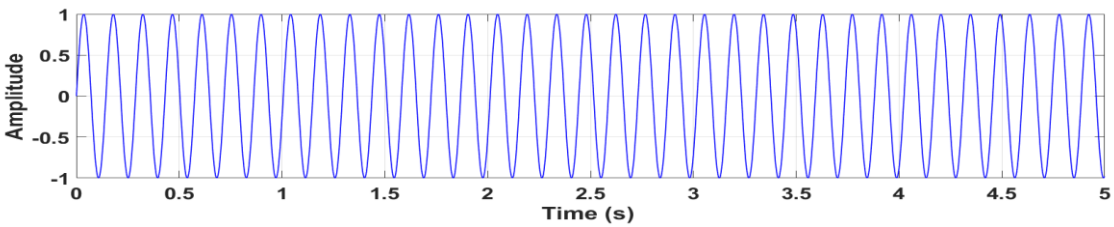

Figure 3.8. Time response of the harmonic input applied in the form of $\cos(\omega t)$

3.2.2.2 Setup Procedures for Investigating the Effect of Location of Attachments

This analysis set utilized a quarter section of the bare plate in order to investigate the effect of attachment location. Since the bare plate is square and clamped along all four edges, symmetry occurs across the quarter sections. The stiffness value of the attachments was taken k = 115.2 N/m. No damping was added to the models. The analysis duration was set to 2.5 seconds. The effect of attachment location was investigated by placing the attachments individually, in pairs, and as 16 attachments. The placement of 16 attachments was carried out both in a regular pattern and randomly.

3.2.2.3 Setup Procedures for Investigating the Effect of Excitation Frequency

In this analysis set, all parameters were kept constant except for the excitation frequency. The stiffness value of the attachments was taken k = 115.2 N/m. No damping was added to the models. The analysis duration was set to 5 seconds. Figures 3.9 to 3.11 show the time domain and frequency domain responses at excitation frequencies of 6.961 Hz, 6.500 Hz, and 14.256 Hz, respectively.

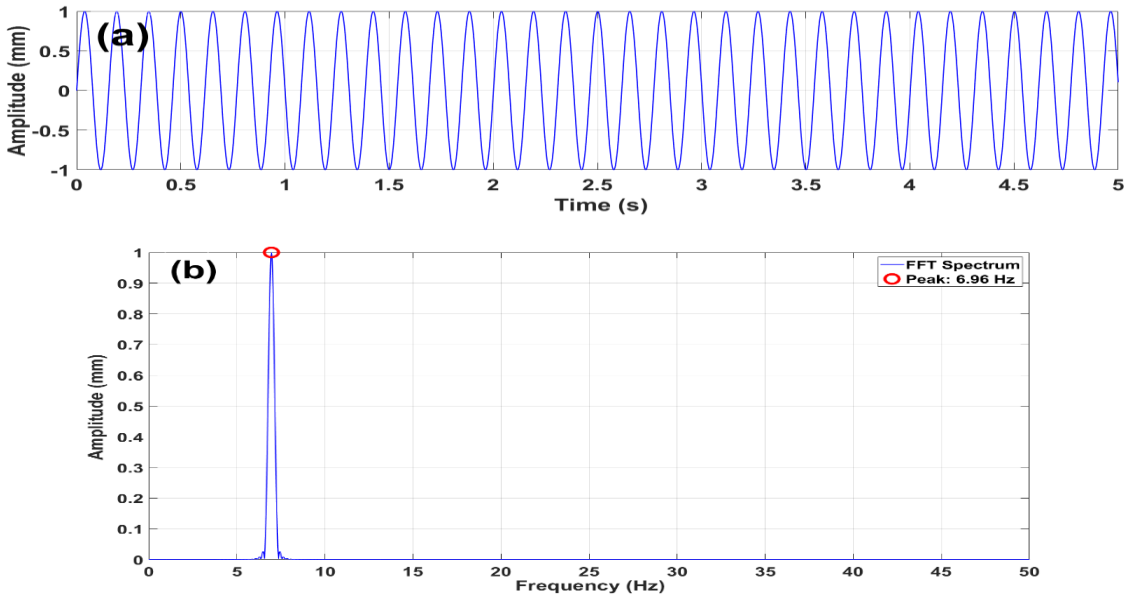

Figure 3.9. a) Time domain and (b) frequency domain responses at 6.961 Hz frequency.

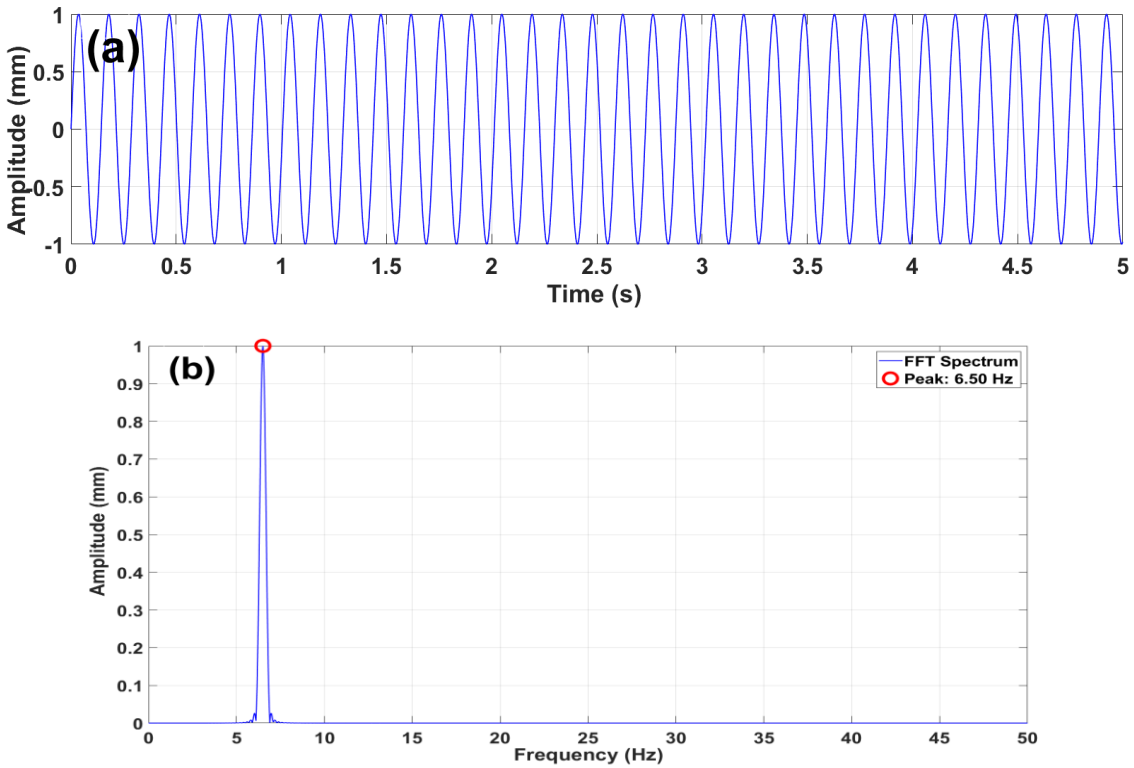

Figure 3.10. a) Time domain and (b) frequency domain responses at 6.500 Hz frequency.

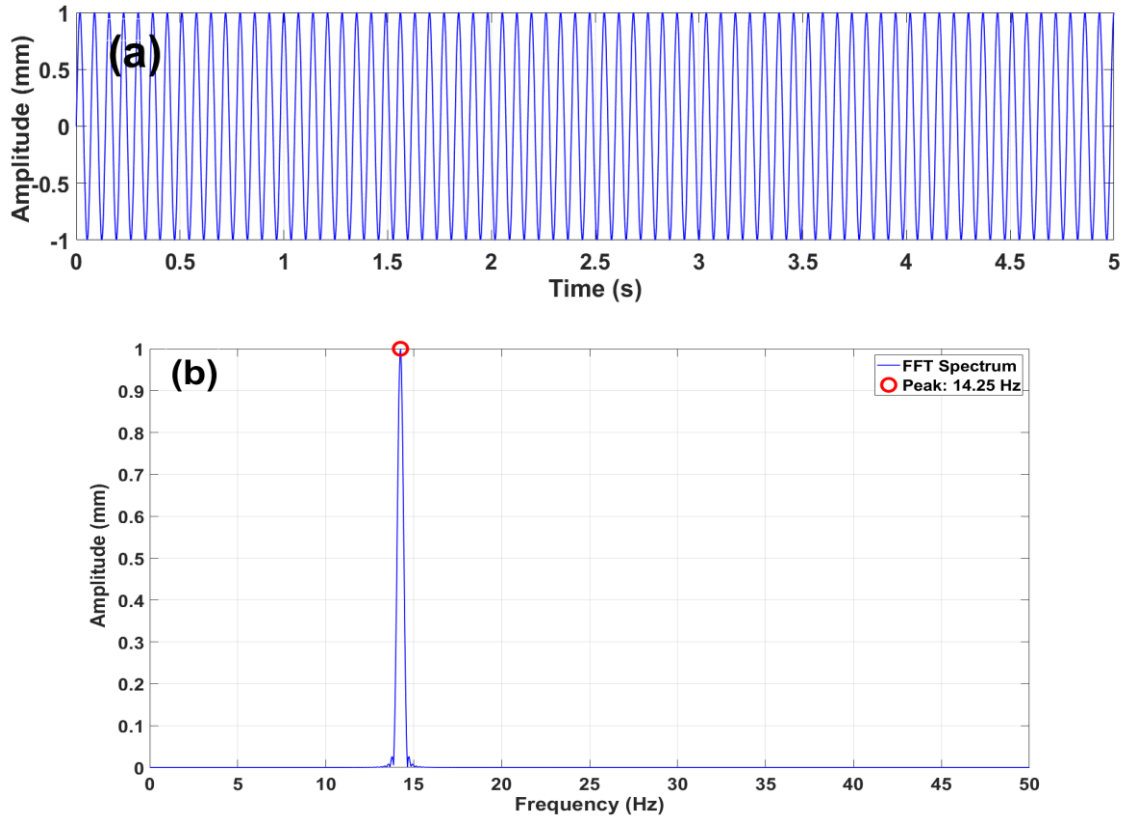

Figure 3.11. a) Time domain and (b) frequency domain responses at 14.256 Hz frequency.

3.2.2.4 Setup Procedures for Investigating the Effect of Damping Ratio

The stiffness value of the attachments was taken k = 115.2 N/m. The analysis duration was set to 3 seconds. In this analysis set, all parameters were kept constant except for the damping ratios. The damping ratios were selected as 0.01, 0.03, 0.05, 0.07 and 0.1. The Rayleigh damping model was used in ANSYS.

3.2.2.5 Setup Procedures for Investigating the Effect of Frequency Ratio

Taking Equation 2.2 into account, it can be seen that two parameters can be used to adjust the frequency ratio: the mass of the attacments and the stiffness of the attachments. The corresponding stiffness values of the attachments for each frequency ratio are given in the Table 3.5.

Table 3.5. Stiffness values of attachments according to frequency ratios.

Frequency ratio	**0,90**	**0,95**	**1,00**	**1,05**	**1,10**
Stiffness of attachments(N/m)	93,3	103,9	115,2	126,9	139,3

In this analysis set, all parameters were kept constant except for the attachments stiffness values. All analyses conducted for different frequency ratios were performed without damping and over a duration of 2,5 seconds. While setting up the analyses for the mass effect, all parameters were kept constant except for the masses of attachments. The corresponding mass values of the single attachment for each frequency ratio are given in the table Table 3.6.

Table 3.6. Mass values of attachments according to frequency ratios.

Frequency ratio	**0,90**	**0,95**	**1,00**	**1,05**	**1,10**
Mass of attachments(kg)	0,0743	0,0663	0,0602	0,0546	0,0498

3.3 Model Verification Based on Coupled Plate-Attachment Systems Reported in the Literature

As mentioned earlier, the simulations we conducted have been carried out using the ANSYS finite element method. To verify the suitability our method, different types of attachments placed on the plate, as reported in studies from the literature, were reconstructed and the results were compared. Comparative analysis results will be presented in the following sequence: plate without attachments, plate with concentrated masses, plate with distributed masses, and finally, plate with mass-spring attachments. The obtained results are presented in the tables under the column labeled present solution.

$$\textbf{Percentage Error} = \frac{\omega_{\text{computed}} - \omega_{\text{reference}}}{\omega_{\text{reference}}} \times 100 \qquad (3.3)$$

The percentage errors between the computed results and reference values were calculated using Equation 3.3, and the corresponding results are summarized in the tables below. The comparison presented in the Table 3.10 was made with respect to the analytical solution provided in the table.

3.3.1 Verification Case for a Plate Without Attachments

In his study, Ramu and Mohanty (2012) calculated the natural frequencies of an isotropic thin plate by varying its thickness using the finite element method and compared the results with the exact Levy-type solution (Ramu and Mohanty (2012). An aluminum plate with dimensions of 0.6 m (width) × 0.4 m (length), with all edges simply supported, was employed for verification. The results for this verification case, involving a plate without attachments, are presented in Table 3.7.

Table 3.7. Results for verification case for a plate without attachments**.**

	Thickness of the plate is 0,00625m		Thickness of the plate is 0,0125m	
Solution Number	FEM solution (Ramu & Mohanty, 2012)	Present solution(Hz)	FEM solution (Ramu & Mohanty, 2012)	Present solution(Hz)
1	135,8	138,41(1.88%)	271,7	275,76(1.47%)
2	259,9	269,12(3.42%)	519,8	535,18(2.87%)
3	417,6	449,75(7.14%)	835,2	893,07(6.47%)
4	466,8	502,44(7.09%)	933,7	996,35(6.28%)
5	535,9	578,14(7.30%)	1071,9	1144,7(6.36%)
6	733,7	807,42(9.13%)	1467,5	1593(7.87%)
7	757,1	864,75(12.44%)	1514,4	1706,6(11.26%)
8	888,3	1056,3(15.90%)	1776,6	2079,6(14.57%)
9	997,8	1163,7(14.25%)	2024,2	2284,8(11.40%)
10	1012,1	1180,6(14.27%)	2263,4	2318,8(2.39%)

3.3.2 Verification Case for a Plate with an Attached Concentrated Mass

Wu and Luo (1997) determined the natural frequencies and corresponding mode shapes of a uniform rectangular plate carrying any number of point masses and translational springs using the analytical and numerical combined method (ANCM). For the verification of model an aluminum plate with a length of 2 meters, a width of 2 meters, and a thickness of 5 milimeters, simply supported on all edges, was used. A concentrated mass of 50 kg was placed at one-quarter of the section of the plate. The results for this verification case, involving a plate with an attached concentrated mass, are presented in Table 3.8.

Table 3.8. Results of verification case for a plate with an attached concentrated mass.

	Natural frequencies (rad/s)				
	ω_1	ω_2	ω_3	ω_4	ω_5
ANCM (Wu & Luo, 1997)	31,814	63,232	95,415	127,616	180,593
Present solution	31,378 (-1.370%)	62,079 (-1.823%)	95,158 (-0.270%)	126,329 (-1.008%)	181,496 (0.497)

3.3.3 Verification Case for a Plate with an Attached Distributed Mass

Kopmaz and Telli (2002) calculated the natural frequencies of a plate carrying a distributed mass using their own developed mathematical approach which was later validated experimentally and numerically by Yıldız and Kopmaz (2017). The characteristics of the coupled systems used in the cases presented in Table 3.9 are summarized as follows. In case 1, a distributed mass with a weigh 195.5 grams was located at the center of one-quarter of the plate, while in case 2, the same mass was placed at the center of the plate. In case 3, a distributed mass with a weigh 720 grams was located at the center of one-quarter of the plate, while in case 4, the same mass was placed at the middle center of the plate. The results of these verification cases for a plate with an attached distributed mass are presented in Table 3.9.

Table 3.9. Results of verification case for a plate with an attached distributed mass.

	CASE 1 (Yıldız & Kopmaz, 2017)		**CASE 2** (Yıldız & Kopmaz, 2017)	
	Experimental results(Hz)	Present solution(Hz)	Experimental results(Hz)	Present solution(Hz)
ω_1	46,5	41,306 (-11.17%)	38,9	34,773 (-10.61%)
ω_2	78,4	75,14 (-4.16%)	88,4	86,041 (-2.66%)
ω_3	110	116,42 (5.51%)	120,8	129,57 (6.76%)
ω_4	142,9	148,95 (4.06%)	125,7	135,13 (6.97%)
ω_5	157,3	163,39 (3.72%)	170,3	177,78 (4.20%)
	CASE 3 (Yıldız & Kopmaz, 2017)		**CASE 4** (Yıldız & Kopmaz, 2017)	
	Experimental results(Hz)	Present solution(Hz)	Experimental results(Hz)	Present solution(Hz)
ω_1	35,2	32,199 (-8.52%)	27,5	24,15 (-12.18%)
ω_2	65,5	62,472 (4.62%)	77,3	83,043 (6.91%)
ω_3	109,1	108,68 (-0.38%)	113,2	116,35 (2.70%)
ω_4	140,5	142,89 (1.67%)	130,6	130,79 (0.14%)
ω_5	161,7	161,25 (-0.27%)	169,4	177,58 (4.60%)

3.3.4 Verification Cases for a Plate with an Attached Mass-Spring Attachments

To evaluate the accuracy of the present model, two separate studies involving plates with mass-spring attachments were reproduced and are presented below as verification cases.

Case 1: Wu et al. (2003), conducted the free vibration analysis of a rectangular plate carrying multiple and various concentrated elements using different methods and compared the results. To verify whether the employed modeling technique is appropriate, identical cases were constructed and examined. In the analysis numbered as 1 in the leftmost column of Table 3.10, a single mass-spring attachment was placed at the point located 1.50 meters along the length and 0.75 meters along the width of the plate. The dimensionless mass ratio was taken as 0.25, and the dimensionless stiffness ratio was set to 0.50. In the analysis numbered as 2 in the leftmost column of Table 3.10, the same plate properties and attachment location as in analysis 1 were used. The dimensionless mass ratio was set to 0.50, and the dimensionless stiffness ratio was set to 1.00.

Case 2: Zhou and Ji (2012) derived the exact solution for the free vibration of thin rectangular plates with discrete spring masses attached using a direct approach and compared their results with previous publications. They obtained the root values in Table 3.11 based on Equation 3.4.

$$\boldsymbol{\Omega = \omega b^2 \sqrt{\frac{\rho h}{D}}} \qquad \textbf{(3.4)}$$

The symbols used in Equation 3.4 correspond to the following definitions: ρ is the mass density per unit volume of the plate; h and D represent the plate's thickness and flexural rigidty, respectively; b is the plate width; ω is the natural frequency; and Ω denotes the dimensionless natural frequency of the plate. The root values in Table 3.11 correspond to the dimensionless natural frequencies given in Equation 3.4. In Table 3.11, the article results are indicated by number 1, the results of the conducted analyses by number 2, and the mode numbers corresponding to the analysis results in the software by number 3.

Table 3.10. Results of verification case-1 plate with an attached mass-spring attachments.

		Natural frequencies (rad/s)				
	Methods	ω_1	ω_2	ω_3	ω_4	ω_5
1	FEM (Wu, Chou, & Chen, 2003)	3,86498	97,87745	160,07677	261,5045	327,29125
	ANCM (Wu, Chou, & Chen, 2003)	3,86492	95,43456	152,68843	248,08642	324,42237
	Analytic solution (Avalos, Larrondo, & Laura, 1993)	3,86505	95,43456	152,68843	248,08641	324,42236
	Present solution	3,86635 (0.03%)	94,77556 (-0.69%)	151,73892 (-0.62%)	248,2235 1(0.05%)	329,2200 6(1.45%)
	Methods	ω_1	ω_2	ω_3	ω_4	ω_5
2	FEM (Wu, Chou, & Chen, 2003)	3,86294	97,89658	160,10008	261,51154	327,30272
	ANCM (Wu, Chou, & Chen, 2003)	3,86282	95,45412	152,71291	248,09395	324,43388
	Analytic solution (Avalos, Larrondo, & Laura, 1993)	3,86306	95,45412	152,71291	248,09395	324,43388
	Present solution	3,86566 (0.06%)	94,78813 (-0.69%)	151,7452 (-0.63%)	248,2235 1(0.05%)	329,2200 6(1.45%)

Table 3.11. Results of verification case-2 plate with an attached mass-spring attachments.

	Dimensionless x location	**Dimensionless y location**	**Dimensionless stiffness ratio**	**Dimension less mass ratio**	**Ω**	**Ω**	**Ω**	**Ω**	**Ω**
1	0,5	0,5	100	0,1	15,81	36,93	102,9	178,8	258,1
			500	0,2	14,23	51,68	117,5	183,4	264,2
			2500	0,5	10,98	55,87	139,0	197,2	282,7
2			100	0,1	3,005	7,020	19,57	33,99	49,08
			500	0,2	2,705	9,825	22,35	34,87	50,23
			2500	0,5	2,087	10,62	26,44	37,49	53,75
3			100	0,1	1	2	7	12	18
			500	0,2	1	4	7	12	18
			2500	0,5	1	4	9	12	18

4. RESULTS

4.1. Effect of Constructional and Controlled Parameters on Energy Transfer

The simulations have been grouped based on six distinct effects. These effects have been evaluated one by one in the analysis of the results. These effects are;

- Effect of number of discrete attachments: All the parameters of the discrete attachments kept constant, only the number of the discrete attachments changed. Kinetic energy and strain energy results are observed according to number of discrete attachment variable.
- Effect of location of discrete attachments: All the parameters of the discrete attachments kept constant, only the location of the discrete attachments changed. Kinetic energy and strain energy results are observed according to location of discrete attachment variable.
- Effect of the variation in the excitation frequency applied to the plate: All the parameters of the discrete attachments kept constant, only excitation frequency changed. Kinetic energy and strain energy are evaluated based on the excitation frequency.
- Effect of the added damping ratio on the coupled system: All the parameters of the discrete attachments kept constant, only damping ratio changed. Kinetic energy and strain energy are evaluated based on the damping ratio.
- Effect of varying the stifness of discrete attachments: All the parameters of the discrete attachments kept constant, only stiffness of the discrete attachments changed. Kinetic energy and strain energy results are observed according to the discrete attachment stifness.
- Effect of varying the mass of discrete attachments: All the parameters of the discrete attachments kept constant, only mass of the discrete attachments changed. Kinetic energy and strain energy are evaluated based on the discrete attachment mass.

4.1.1 Effect of Number of Discrete Attachments on Energy Transfer

Simulations have been carried out with different values of number of discrete attachment. The total energies obtained according to the number of discrete attachments and the energies per unit discrete attachment are shown in the Table - 4.1. It was observed that the total energy mainly composed of the kinetic energy.

Table 4.1. Total energy and energy per unit attachment values versus different number of discrete attachment.

Number of Attachment	Total Energy (Joule)	Energy per Unit Attachment (Joule)
2	89,028399	44,514199
4	177,760070	44,440017
8	468,927534	58,615941
12	717,468918	59,789076
16	1143,862056	71,491378
24	1768,061774	73,669240
32	2320,280554	72,508767
36	2816,246642	78,229074
40	3001,590877	75,039772
48	3633,883013	75,705896
64	4384,563370	68,508802

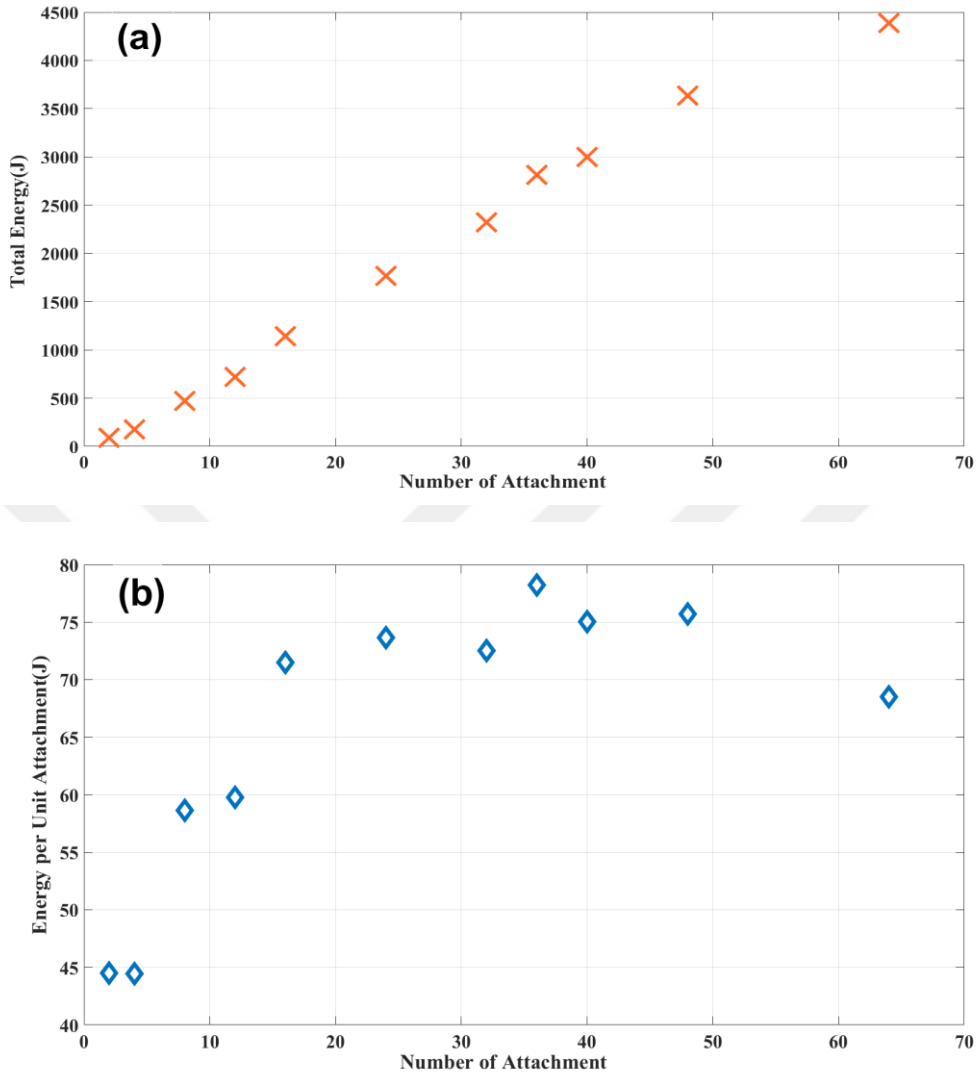

Figure 4.1. a) Total energy for different numbers of attachments b) Energy per unit attachment for different numbers of attachments.

It is observed that the total energy increases as more discrete attachments are added to structure, as shown in Figure 4.1(a). This is because the discrete attachments possess a certain mass, and as the plate vibrates, the attachments also vibrate, thereby contributing additional kinetic energy. Therefore, increasing the number of attachments on a vibrating plate generates more energy. In Figure 4.1(b) it is observed that the energy per unit discrete attachment increases up to 36 attachments after that point the energy per unit discrete attachment decreases . This trend can be explained by the fact that, as the number of attachments increases, more of them are located near the edges of the plate.

As a result, the energy contribution per attachment starts to decline beyond a certain number of attachments.

4.1.2 Effect of Location of Discrete Attachments on Energy Transfer

The effect of attachment location was investigated using three different numbers of discrete attachments. Due to the use of constant number of discrete attachments, the analysis focused solely on the total kinetic and strain energy.

4.1.2.1 Effect of the Location of a Single Attachment

The plate has been divided into four equal symmetrical regions. Since the plate is square, a quarter region has been used, and this region has been divided into 16 equal cells. A single attachment has been placed at the center of a different cell each time, and analysis result have been obtained accordingly. Consistent with Figure 3.1 in the previous section, the location of a single attachment on the plate is represented by xa and ya, where *a* and *b* denote the length and width of the plate in the x and y directions, respectively. Total energy results for different layouts of a single discrete attachment are presented in Table 4.2.

Table 4.2. Total energy results for different layouts of a single attachment.

Location (m) $[x_a, y_b]$	Total Energy(mJ)	Location (m) $[x_a, y_b]$	Total Energy(mJ)	Location (m) $[x_a, y_b]$	Total Energy(mJ)	Location (m) $[x_a, y_b]$	Total Energy(mJ)
0,1 0,7	265,4436	**0,1 0,5**	153,52570	**0,1 0,3**	37,469036	**0,1 0,1**	1,1280103
0,3 0,7	8404,5986	**0,3 0,5**	4892,6638	**0,3 0,3**	1221,5453	**0,3 0,1**	37,851008
0,5 0,7	33881,811	**0,5 0,5**	19560,954	**0,5 0,3**	4975,8354	**0,5 0,1**	157,05889
0,7 0,7	60551,478	**0,7 0,5**	34425,741	**0,7 0,3**	8764,5214	**0,7 0,1**	279,68834

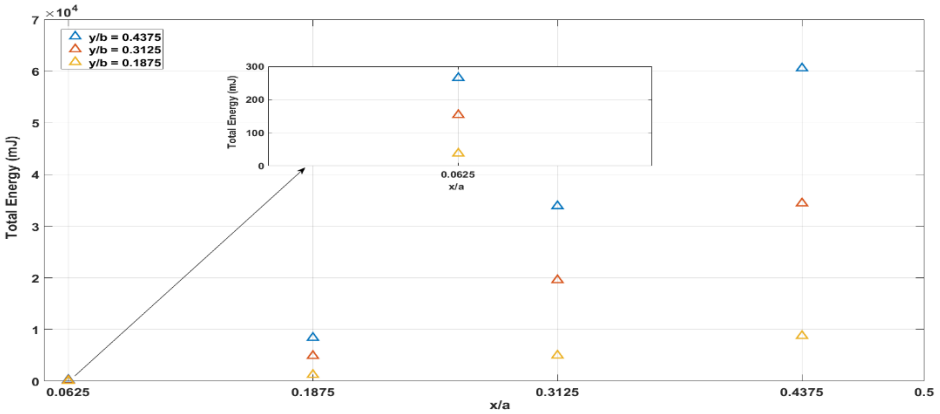

Figure 4.2. Energy values based on the placement of a single discrete attachment.

Based on the results illustrated in Figure 4.2, it has been observed that the total energy collected by a single attachment increases as its position shifts from the plate edges toward the center. Since all four edges of the plate are fixed and the excitation is applied at the center, higher enery levels occur near the central region. Therefore, single discrete attachment located closer to the center accumulate more energy.

4.1.2.2 Effect of the Locations of Two Discrete Attachments

As mentioned earlier, the plate has been divided into symmetrical regions for these two attachment configurations, and the attachments have been placed at the centers of the each cell. In this section, the attachments have been placed in both diagonal and vertical configurations during the analyses. Total energy results for vertical and diagonal layouts of two discrete attachments are presented in Table 4.3.

Table 4.3. Total energy results for vertical and diagonal layouts of two discrete attachments.

Simulation Number	Diagonal Configuration Total Energy(J)	Vertical Configuration Total Energy(J)
1	41,9499	1,6458
2	16,2735	5,1264
3	34,0567	9,7861
4	24,1451	31,1965
5	9,5771	53,5473

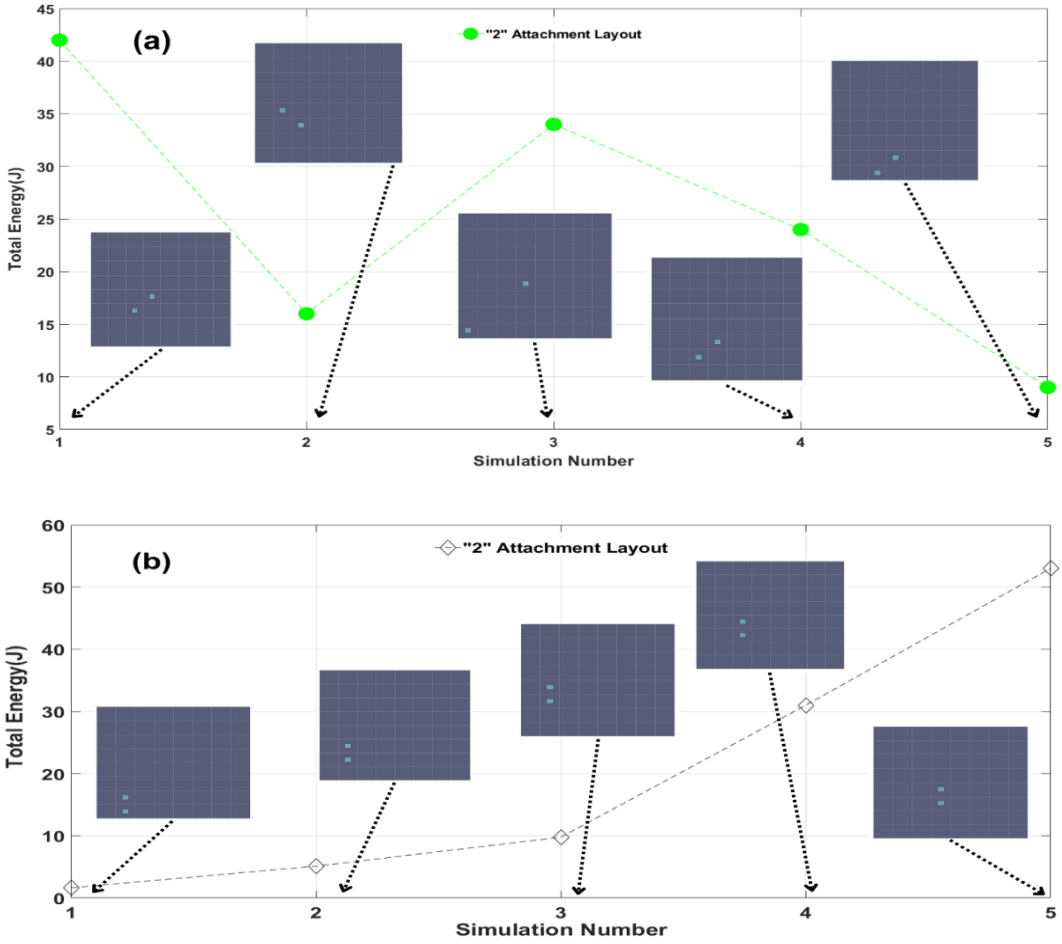

Figure 4.3. a) Total energy (diagonal configuration) of two discrete attachments b) Total energy (vertical configuration) of two discrete attachments.

Figure 4.3(a) shows that simulation number 1 yields the highest energy, whereas simulation number 5 results in the lowest. Figure 4.3(b) illustrates a progressive increase in the accumulated energy from simulation 1 through simulation 5. A common observation in both diagonal and vertical placement configurations is that the accumulated energy increases as the attachments are positioned closer to the central regions of the plate, and decreases when they are placed near the edges – an outcome also observed previously in the single attachment placement results.

4.1.2.3. Effect of the Random Placement of 16 Discrete Attachments

This section has investigated the energy values of 16 attachments, which have been placed both in an organized pattern and in random configurations. Total energy results of 16 attachments for organized and random layouts are presented in Table 4.4.

Table 4.4. Total energy results 16 attachments organized and random placement.

Simulation Number	Organized Configuration Total Energy(J)	Random Configuration Total Energy(J)
1	563,966473	352,409732
2	29,277977	339,158475
3	297,782811	337,488127
4	175,559723	337,506851
5	447,397220	353,639660

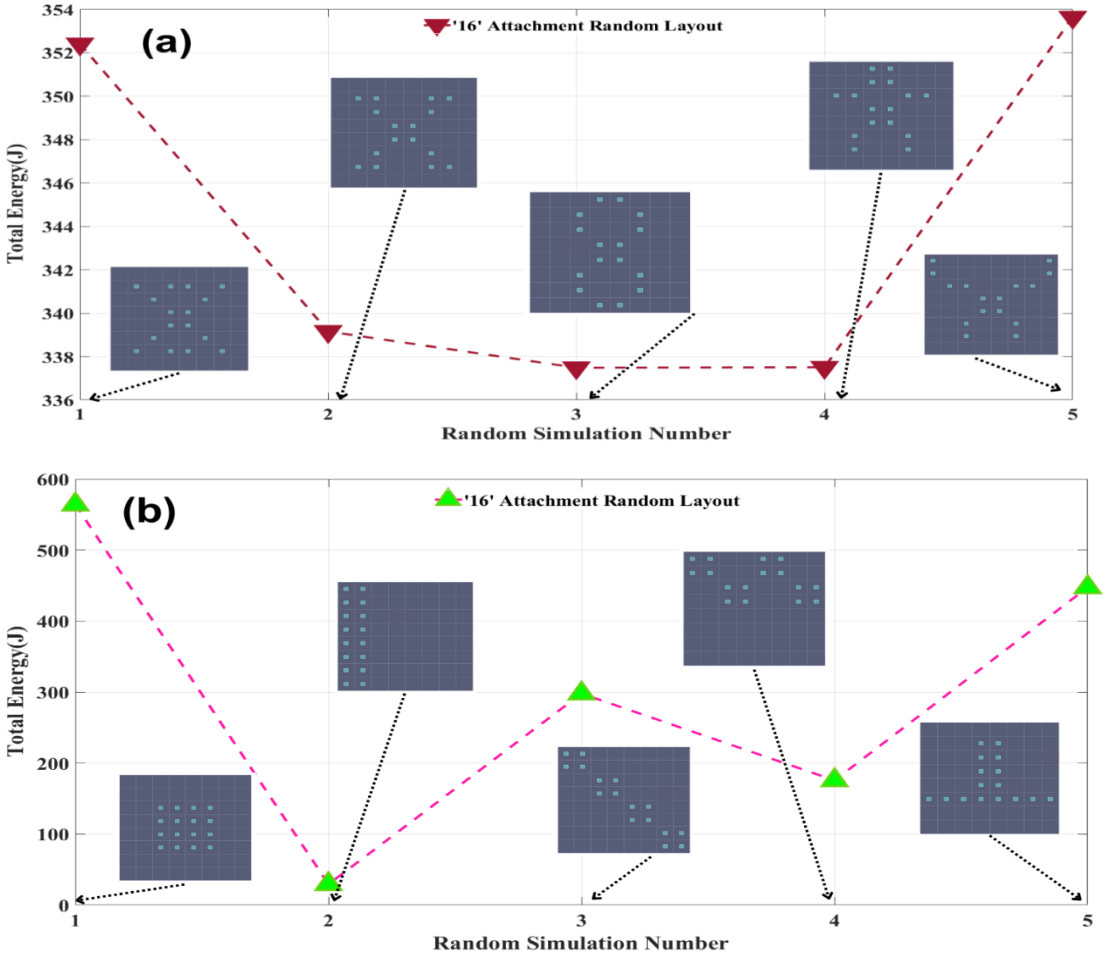

Figure 4.4. a) Total energy (random configuration) for 16 attachments b) Total energy (organized random configuration) for 16 attachments.

Figure 4.4(a) presents a completely random placement of attachments, while Figure 4.4(b) shows a randomized distribution constrained within a predefined pattern. When examining the graph of the random placement results, it is observed that the energy values are scattered between 330 and 360 joules. This can be attributed to the fact that, in these configurations, four attachments remain fixed at the center, while the others are distributed around the central region. As seen in Figure 4.4(b), similar to the previously obtained results, the highest energy is observed in the attachments located at the center of the plate, while the lowest energy is recorded in those positioned near the edges.

4.1.3. Effect of the Variation in the Excitation Frequency Applied to the Plate on Energy Transfer

In this thesis the plate is considered as the source of vibration. Initially, the plate is rest. Afterward, the plate is subjected to excitation at a specific frequency to generate vibrations. As excitation frequencies, the first mode frequency of the plate 6.961 Hz, a frequency close to the first mode 6.500 Hz, and the second mode frequency 14.256 Hz have been used.

4.1.3.1. Effect of the First Mode-Based Excitation

In the previous analyses focusing on the number of attachments, the plate had already been using its first mode frequency. Table 4.5 shows the total energy values obtained after excitation with the bare plate's first mode frequency and at a frequency close to the first mode frequency. The energy results per unit of attachment are also given in the same table.

Table 4.5. Total energy and energy per unit attachment results for the first mode-based excitation versus near the first mode-based excitation.

	First Mode Results	**Near the First Mode Results**
Number of Attachment	Total Energy (Joule)	Total Energy (Joule)
2	89,028398	2,13346
4	177,76007	4,284981
8	468,927533	11,50772
12	717,468918	17,910334
16	1143,862056	29,063154
24	1768,061774	46,919006
32	2320,280554	65,865152
36	2816,246642	82,409893
40	3001,590877	90,863684
48	3633,883013	121,165558
64	4384,56337	185,895396
	First Mode Results	**Near the First Mode Results**
Number of Attachment	Enery per Unit Attachment (Joule)	Enery per Unit Attachment (Joule)
2	44,514199	1,066734
4	44,440017	1,071245
8	58,615941	1,438465
12	59,789076	1,492527
16	71,491378	1,816447
24	73,66924	1,954958
32	72,508767	2,058286
36	78,229073	2,289163
40	75,039771	2,271592
48	75,705896	2,524282
64	68,508802	2,904615

4.1.3.2. Effect of the Near First Mode-Based Excitation

The analyses have been repeated by setting the excitation frequency to 6.500 Hz. Table 4.5 summarizes the total energy obtained from the simulations, along with the corresponding energy per discrete attachment, for the case where the excitation frequency is set to 6.500 Hz and 6.961 Hz. These values are used to assess the influence of excitation frequency on energy distribution.

While the highest total energy under first mode excitation reaches 4384 joules for 64 attachments, this value drops significantly to 185 joules when the plate is excited at a frequency close to the first mode. A comparison of the two results reveals that first mode excitation yields nearly 24 times more energy than excitation near the first mode. This result is not surprising. This is because the plate and the discrete attachments are effectively coupled at the first mode frequency. When examining the energy per attachment, it is observed that for 2 and 24 attachments, the energy values range between 1 and 2 joules, whereas for 32 and 64 attachments, the values range between 2 and 3 joules. This reduction can also be atttibuted to the fact that a important portion of the energy is absorbed by the plate. The energy values are also presented graphically Figure 4.5.

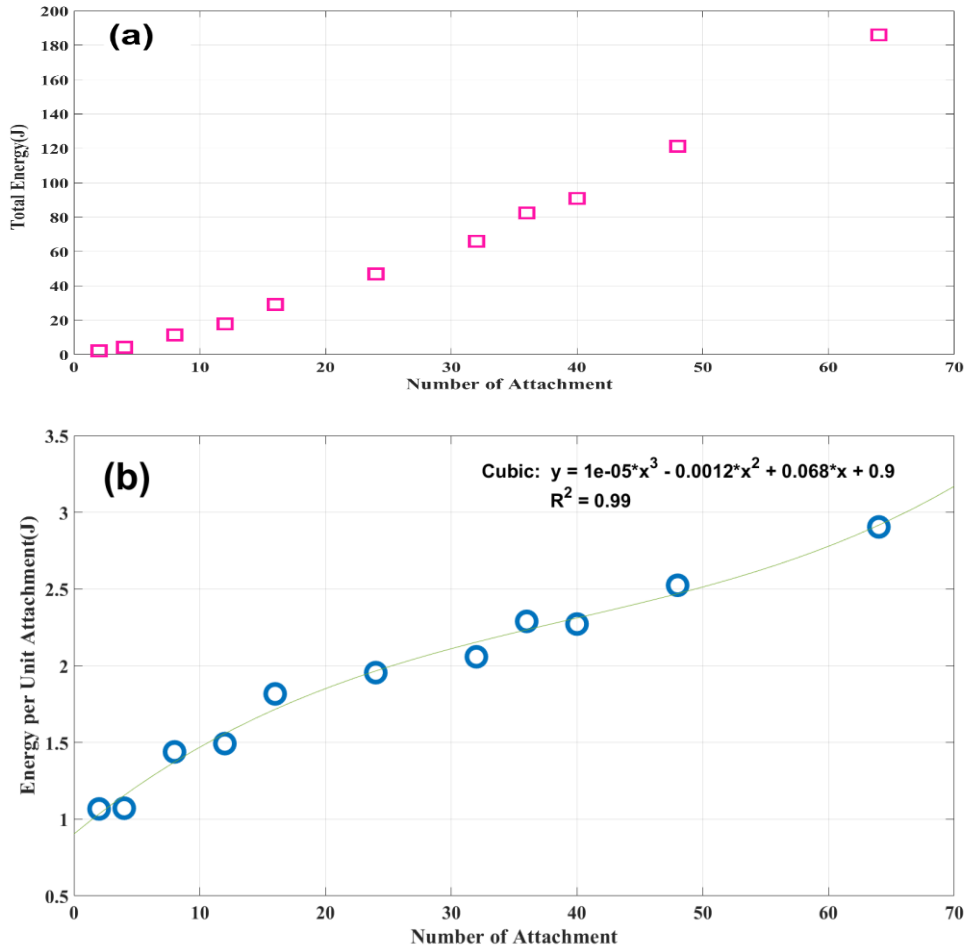

Figure 4.5. a) Total energy for the near first mode-based excitation b) Energy per unit attachment for the near first mode-based excitation.

4.1.3.3. Effect of the Second Mode-Based Excitation

To investigate the effect of higher mode excitaton, the analyses were repeated using the second mode frequency of the plate (14.256 Hz) as the input. Table 4.7 shows the total energy values obtained after excitation with the bare plate's first mode frequency and second mode frequency. The energy results per unit of attachment are also given in the same table.

Table 4.6. Total energy and energy per unit attachment results for the first mode-based excitation versus second mode excitation.

	First Mode Results	**Second Mode Results**
Number of Attachment	Total Energy (Joule)	Total Energy (Joule)
2	89,028398	0,074599
4	177,76007	0,148884
8	468,927533	0,355319
12	717,468918	0,581761
16	1143,862056	0,675326
24	1768,061774	1,089847
32	2320,280554	1,515442
36	2816,246642	1,685407
40	3001,590877	2,18714
48	3633,883013	3,235968
64	4384,56337	5,057533
	First Mode Results	**Second Mode Results**
Number of Attachment	Enery per Unit Attachment (Joule)	Enery per Unit Attachment (Joule)
2	44,514199	0,037299
4	44,440017	0,037221
8	58,615941	0,044414
12	59,789076	0,04848
16	71,491378	0,042207
24	73,66924	0,04541
32	72,508767	0,047357
36	78,229073	0,046816
40	75,039771	0,054678
48	75,705896	0,067416
64	68,508802	0,079023

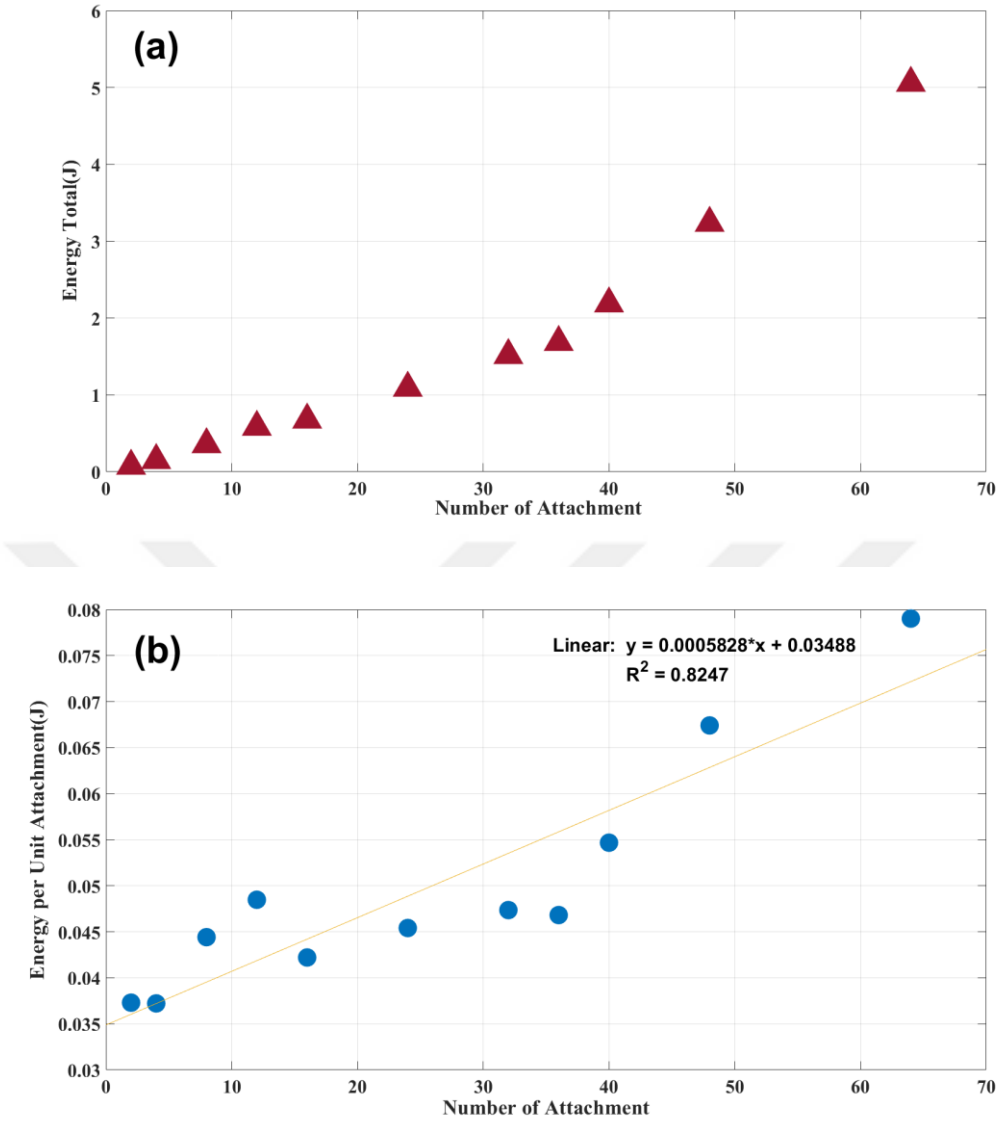

Figure 4.6. a) Total energy for the second mode-base excitation b) Energy per unit attachment for the second mode-based excitation.

Considering Table 4.6 and Figure 4.6 the overall effect of excitation frequency can be evaluated as follows: the highest total energy is obtained when the system is excited at the first mode frequency. The lowest total energy is observed under second mode excitation, while the results for excitation near the first mode frequency lie between these two extremes. A similar trend is also valid for the energy per discrete attachments.

4.1.4. Effect of the Added Damping Ratio on Energy Transfer in a Coupled System

The analyses provided up to this point, presented in the form of tables and graphs, have been performed without the inclusion of any damping in the system. However, energy dissipation is inevitable in practical applications due to various factors. In this section, small amounts of damping are introduced to examine its impact on the system. In Table 4.8 the symbol 'ζ' is used to represent the damping ratios. Total energy and energy per unit attachment results obtained by adding small amounts of damping to the attachments are presented in Table 4.8. Additionally, the visualized results are presented in Figure 4.7. Here, N.A refers to the number of attachments.

Table 4.7. Total energy and per unit attachments results with small amounts of damping.

	Total Energy (Joule)					
N.A	$\zeta = 0$	$\zeta = 0{,}01$	$\zeta = 0{,}03$	$\zeta = 0{,}05$	$\zeta = 0{,}07$	$\zeta = 0{,}1$
2	11,2386	5,75970	2,04990	0,97925	0,56172	0,30020
4	22,4477	11,5072	4,09660	1,95716	1,12271	0,60004
8	59,2855	30,3508	10,8117	5,16904	2,96768	1,58864
12	90,9341	46,5683	16,6014	7,93998	4,55959	2,44146
16	145,368	74,3042	26,504	12,6850	7,29007	3,90900
24	226,754	116,160	41,5192	19,8914	11,4381	6,13640
32	302,442	155,359	55,7006	26,7267	15,3794	8,25294
36	369,949	190,108	68,2494	32,7779	18,8731	10,1348
40	397,677	204,657	73,5866	35,3689	20,3723	10,9416
48	501,390	258,422	93,240	44,9189	25,9112	13,9344
64	639,599	332,423	121,471	58,9834	34,1760	18,43605

	Energy per Unit Attachment (Joule)					
N.A	$\zeta = 0$	$\zeta = 0{,}01$	$\zeta = 0{,}03$	$\zeta = 0{,}05$	$\zeta = 0{,}07$	$\zeta = 0{,}1$
2	5,61930	2,87985	1,02495	0,48962	0,28086	0,15010
4	5,61194	2,87680	1,02415	0,48929	0,28067	0,15001
8	7,41069	3,79385	1,35147	0,64613	0,37096	0,19858
12	7,57784	3,88069	1,38345	0,66166	0,37996	0,20345
16	9,08550	4,64401	1,65654	0,79281	0,45562	0,24431
24	9,44809	4,84004	1,72996	0,82880	0,47659	0,25568
32	9,45132	4,85499	1,74064	0,83521	0,48060	0,25790
36	10,2763	5,28079	1,89581	0,91049	0,52425	0,28152
40	9,94193	5,11643	1,83966	0,88422	0,50930	0,27354
48	10,4456	5,38379	1,94251	0,93584	0,53981	0,29031
64	9,99374	5,19412	1,89798	0,92161	0,53400	0,28806

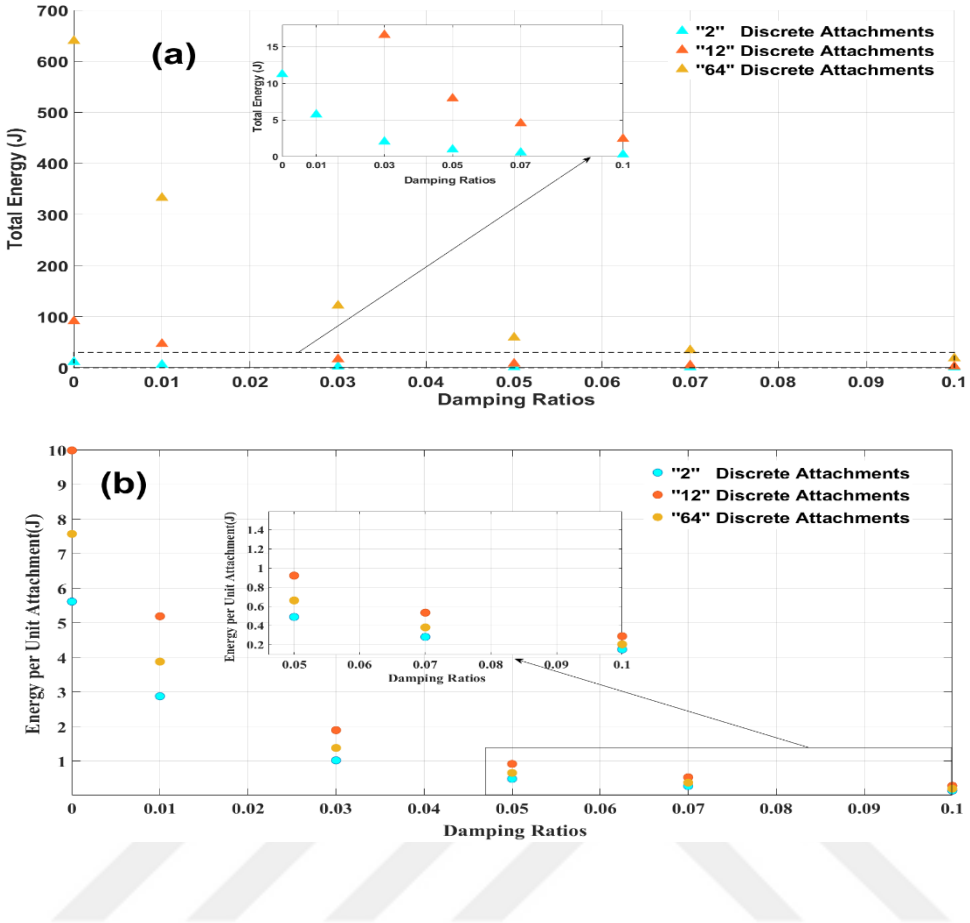

Figure 4.7. a) Total energy results with small amounts of damping b) Energy per unit attachment results with small amounts of damping.

The Rayleigh damping method used in ANSYS was applied when adding the damping ratio. In the program's settings, the frequency value, which is the first mode frequency of the plate (6,961 Hz), was entered to remain constant in all analyses. The damping ratio section was filled with the corresponding value depending on which damping ratio was to be applied. It is calculated the stiffness coefficient based on these values. Since the mass coefficient's effect on the results is insignificant, the program automatically sets its value to 0.

To examine the effect of damping, attachments with 2, 16, and 64 units have been chosen. For all selected attachment numbers, an increase in the damping ratio leads to a gradual decrease in the energy values. Similar trends have been observed when the values for other attachment numbers in the table are examined.

As the damping ratio increases, the vibrations in the system are damped more quickly. This means that the vibrating structure loses its energy rapidly, leading to a decrease in the total energy value.

4.1.5. Effect of Varying the Stiffness of Discrete Attachments on Energy Transfer

In order to examine the influence of the frequency ratio, all other parameters have been kept constant while the frequency ratios have been systematically varied. While the plate's frequency remains constant at 6.961 Hz, the frequency of the attachments was adjusted according to Equation 3.2. During this adjustment, the mass of the attachments was kept constant, and their stiffness values were set based on the values given in Table-3.5. Results of total energy and energy per unit attachment for varying stiffness values are presented in Table 4.9.

Table 4.8. Results of total energy and energy per unit attachment for varying stiffness values.

	Total Energy (Joule)				
N.A	F.R = 0,9	F.R = 0,95	F.R = 1	F.R = 1,05	F.R =1,1
2	0,422398482	2,116228937	11,23861844	3,014254022	0,856494546
4	0,841122955	4,181378064	22,44777652	6,113006725	1,721294648
8	2,224643373	10,84677431	59,28555879	16,59371499	4,562181524
12	3,394322161	16,2753329	90,93413441	26,27930022	7,077006943
16	5,435504567	25,68520132	145,3680183	42,8581455	11,31685753
24	8,396255296	38,54356989	226,7543358	71,09028611	18,04212924
32	11,04187861	48,91361519	302,4424004	103,0152635	24,87107743
36	13,50409255	59,24767802	369,9492809	129,3047411	30,65574849
40	14,41484914	62,12725826	397,6772772	144,2283287	33,42135532
48	18,13310473	76,64665419	501,3908538	193,1559708	42,97276191
64	22,7211987	89,37599245	639,5992655	300,6231702	59,43383413

	Energy per Unit Attachment (Joule)				
N.A	F.R = 0,9	F.R = 0,95	F.R = 1	F.R = 1,05	F.R = 1,1
2	0,211199241	1,058114468	5,619309219	1,507127011	0,428247273
4	0,210280739	1,045344516	5,611944129	1,528251681	0,430323662
8	0,278080422	1,355846788	7,410694848	2,074214374	0,57027269
12	0,28286018	1,356277742	7,577844534	2,189941685	0,589750579
16	0,339719035	1,605325082	9,085501144	2,678634094	0,707303596
24	0,349843971	1,605982079	9,448097323	2,962095254	0,751755385
32	0,345058706	1,528550475	9,451325014	3,219226983	0,77722117
36	0,375113682	1,645768834	10,27636891	3,591798365	0,851548569
40	0,360371228	1,553181457	9,941931931	3,605708218	0,835533883
48	0,377773015	1,596805296	10,44564279	4,024082726	0,895265873
64	0,35501873	1,396499882	9,993738524	4,697237034	0,928653658

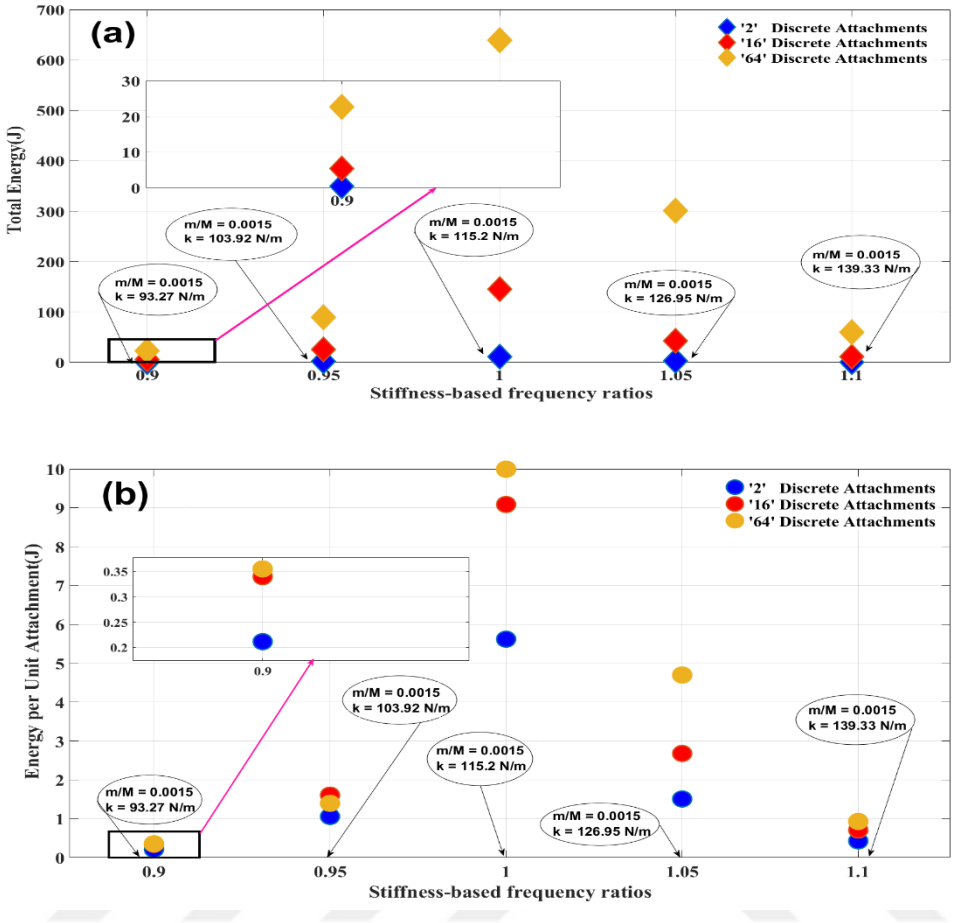

Figure 4.8. a) Total energy for different stiffness values b) Energy per unit attachment for different stiffness values.

As observed in Figures 4.8(a) and (b), the energy values increase as the frequency ratio approaches 1, reaching their maximum at a ratio 1. Beyond this point, the energy begins to decrease with increasing frequency ratio. Despite the uniform increments in frequency ratio, the resulting energy values are not symmetric. This outcome is to be excepted. Recall that the frequency equation states that the frequency value is proportional to square root of the stiffness value. It can be observed that figures a ve b show similar trend. However, when considering the selected attachment values, it is observed that the energy values per unit attachment for 16 and 64 attachments are close to each other. It can be seen that 16 attachments might be more effective when designing a lighter system. The natural frequencies in the coupled system and the variation of the frequency ratio have an effect on energy transfer, and this is presented in this section. The coupled natural frequency results of the plate and attachments are presented in Table 4.10. Figure 4.9 presents the natural frequencies of the bare plate and the plate with selected

attachments. The first and second, third and fourth, and fifth and sixth mode shapes of the plate with two discrete attachments are presented in Figures 4.10, 4.11, and 4.12, respectively.

Table 4.9. Coupled natural frequencies of the plate and attachments.

	w1	w2	w3	w4	w5	w6
2	6,7894	6,9605	7,0646	14,024	14,109	20,765
4	6,7432	6,9587	6,9587	6,9609	7,1235	14,037
8	6,6665	6,9534	6,9561	6,9602	6,9613	6,9618
12	6,6251	6,9486	6,9517	6,9587	6,96	6,9612
16	6,6937	6,9453	6,9477	6,958	6,9597	6,9599
24	6,5603	6,9361	6,9384	6,9555	6,9564	6,9582
32	6,4526	6,9233	6,9258	6,9497	6,9524	6,9563
36	6,2911	6,9136	6,9193	6,949	6,9513	6,952
40	6,2876	6,9094	6,9164	6,9461	6,9492	6,9549
48	6,1218	6,8926	6,8944	6,9375	6,9457	6,9471
64	6,0027	6,865	6,873	6,9276	6,9388	6,9401

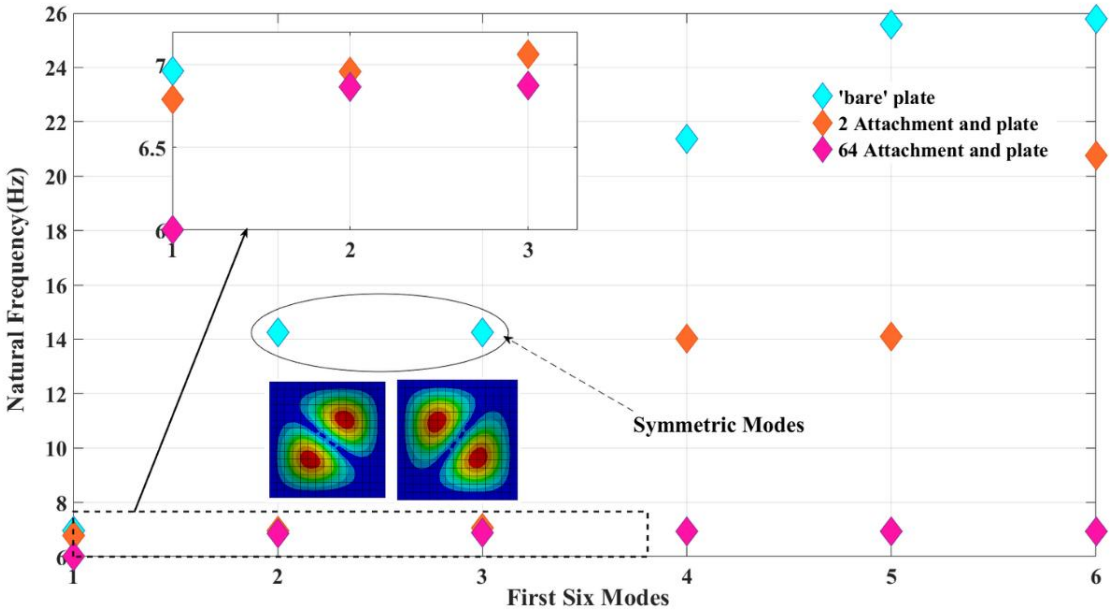

Figure 4.9. Natural frequencies of the bare plate and the plate with selected attachments.

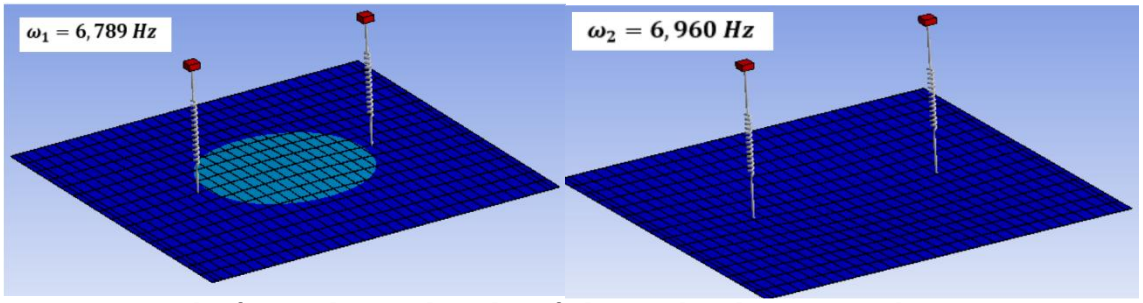

Figure 4.10. The first and second modes of plate with 2 discrete attachments.

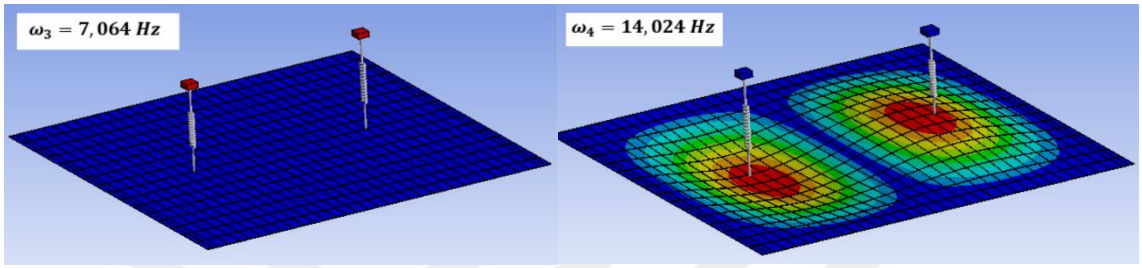

Figure 4.11. The thirth and fourth modes of plate with 2 discrete attachments.

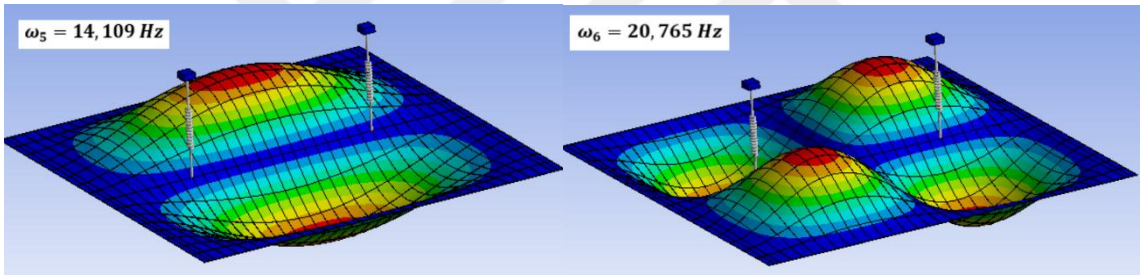

Figure 4.12. The fifth and sixth modes of plate with 2 discrete attachments.

Based on the obtained results, it has been observed that the highest natural frequency values occur in the bare plate, and the natural frequencies decrease as the number of attachments on the plate increases. During these simulations, the attachments were coupled with the plate at its first natural frequency. Therefore, the frequency ratio has been taken as 1. The results obtained for different frequency ratios are presented in the Table 4.11 and Figure 4.13.

The frequency ratios were adjusted by varying the stiffness values while keeping the masses of the attachments constant. The stiffness values used were taken from Table 3.5. It is observed that as the frequency ratio increases, the coupled natural frequencies also increase.

Table 4.10. Natural frequencies of some attachments at different frequency ratios.

	w1	w2	w3	w4	w5	w1	w2	w3	w4	w5
F.R	2 Discrete Attachments and Plate					8 Discrete Attachments and Plate				
0,9	6,2438	6,2635	6,9133	14,024	14,109	6,1752	6,2586	6,2605	6,2632	6,2641
0,95	6,5651	6,6112	6,9396	14,024	14,109	6,4557	6,6053	6,6075	6,6109	6,6119
1	6,7894	6,9605	7,0646	14,024	14,109	6,6665	6,9534	6,9561	6,9602	6,9613
1,05	6,8481	7,3065	7,3519	14,024	14,109	6,7839	7,2981	7,3013	7,3062	7,3075
1,1	6,8629	7,6541	7,6848	14,025	14,109	6,8413	7,644	7,6479	7,6538	7,6554
F.R	16 Discrete Attachments and Plate					64 Discrete Attachments and Plate				
0,9	6,1368	6,253	6,2546	6,2617	6,2629	5,6794	6,1974	6,2027	6,24	6,2479
0,95	6,4295	6,5985	6,6005	6,6091	6,6105	5,8565	6,5315	6,5381	6,5833	6,5928
1	6,6937	6,9453	6,9477	6,958	6,9597	6,0027	6,865	6,873	6,9276	6,9388
1,05	6,9113	7,2884	7,2913	7,3037	7,3057	6,119	7,1929	7,2026	7,2681	7,2813
1,1	7,0753	7,6326	7,6362	7,6509	7,6532	6,2117	7,5194	7,5313	7,6094	7,6249

In Table 4.11, F.R corresponds to the frequency ratio.

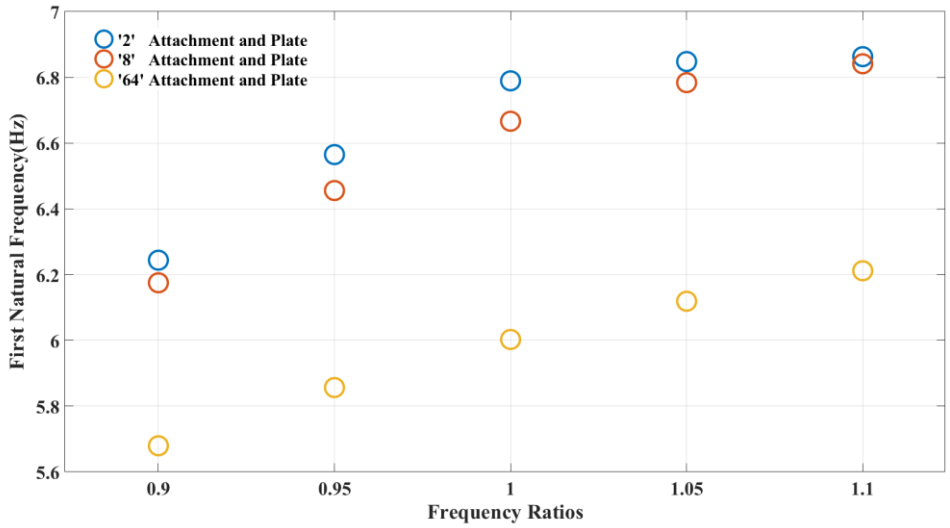

Figure 4.13. The first mode natural frequencies of some discrete attachments.

4.1.6. Effect of Varying the Mass of Discrete Attachments on Energy Transfer

In this section, similar to previous one, frequency ratios have been considered. However, in this part, the mass values of the attachments have been changed to evaluate the effect of mass..The frequency ratios were adjusted by varying the mass values while keeping the stiffness values of the attachment constant. The mass values used were taken from Table 3.6. Results of total energy and energy per unit attachment for varying mass values are presented in Table 4.12 and Figure 4.14. In Table 4.12, F.R corresponds to the frequency ratio.

Table 4.11. Results of total energy and energy per unit attachment for varying mass values.

	Total Energy (Joule)				
N.A	F.R = 0,9	F.R = 0,95	F.R = 1	F.R = 1,05	F.R = 1,1
2	0,523772727	2,78797491	11,23861844	2,708826365	0,696472952
4	1,042030605	5,503053713	22,44777652	5,486427007	1,398766051
8	2,750694036	14,24187772	59,28555879	14,85313144	3,702408399
12	4,188477331	21,32123666	90,93413441	23,45992109	5,737582815
16	6,696886219	33,58528447	145,3680183	38,18458252	9,166870113
24	10,30353023	50,17165938	226,7543358	63,03286363	14,5951567
32	13,47605063	63,27036803	302,4424004	90,80328364	20,09449678
36	16,45483319	76,50149215	369,9492809	113,7821273	24,78193482
40	17,51507226	79,95624472	397,6772772	126,6060457	27,00026493
48	21,94860346	98,2277842	501,3908538	168,9604171	34,73799749
64	27,10471657	112,645357	639,5992655	260,5921738	47,94251803

	Energy per Unit Attachment (Joule)				
N.A	F.R = 0,9	F.R = 0,95	F.R = 1	F.R = 1,05	F.R = 1,1
2	0,261886363	1,393987455	5,619309219	1,354413182	0,348236476
4	0,260507651	1,375763428	5,611944129	1,371606752	0,349691513
8	0,343836755	1,780234715	7,410694848	1,85664143	0,46280105
12	0,349039778	1,776769722	7,577844534	1,954993424	0,478131901
16	0,418555389	2,099080279	9,085501144	2,386536408	0,572929382
24	0,42931376	2,090485808	9,448097323	2,626369318	0,608131529
32	0,421126582	1,977199001	9,451325014	2,837602614	0,627953024
36	0,4570787	2,125041449	10,27636891	3,160614646	0,688387078
40	0,437876807	1,998906118	9,941931931	3,165151142	0,675006623
48	0,457262572	2,046412171	10,44564279	3,520008689	0,723708281
64	0,423511196	1,760083703	9,993738524	4,071752716	0,749101844

Based on the results obtained, it has been observed that the influence of the mass of discrete attachments on the system's energy response exhibits a trend similar to that of the stiffness variations. Although mass and stiffness affect the dynamic behavior of the system in different ways, their impact on the energy accumulation follows a comparable pattern – particularly around the frequency ratio of 1.

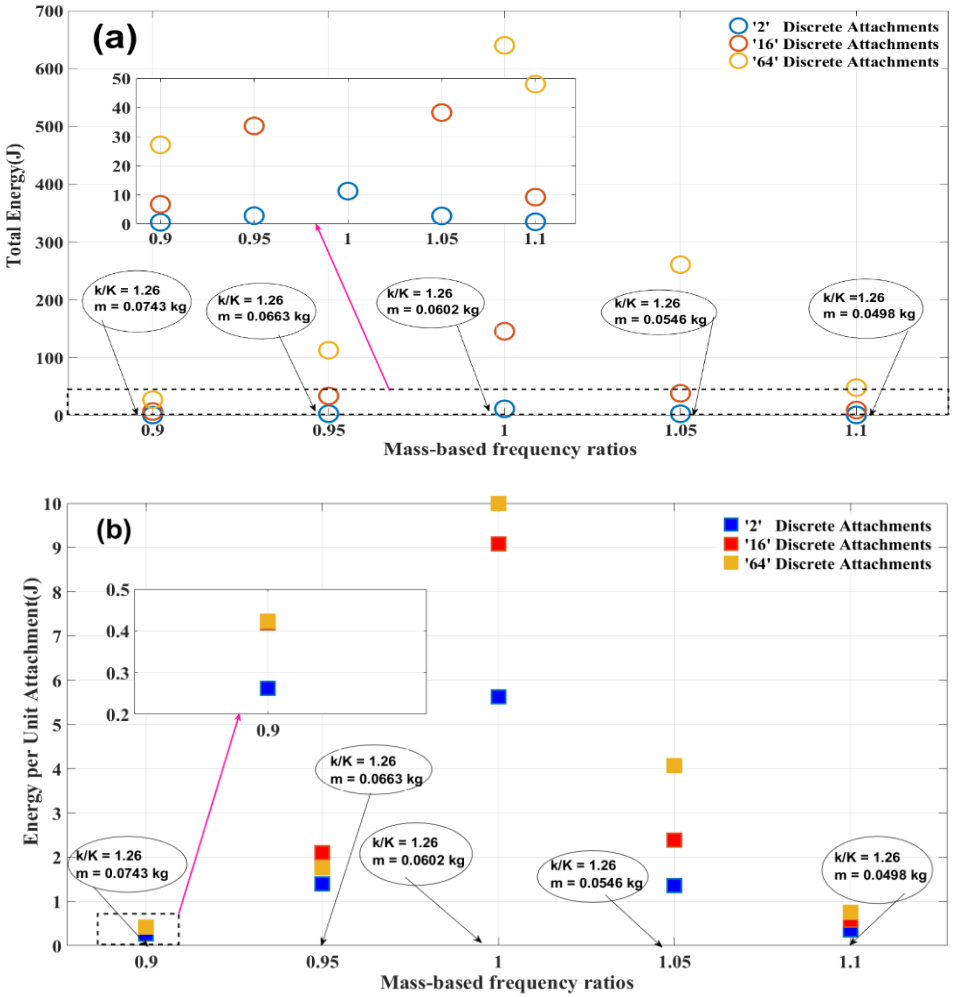

Figure 4.14. a) Total energy for different mass values b) Energy per unit attachment for different mass values.

This similarity can be attributed to the fact that both parameters play a crucial role in tuning the resonance between the primary structure and attachments, thereby affecting the energy transfer efficiency. When the frequency ratios of 0.90 and 0.95 are selected, the influence of mass appears to dominate, whereas at frequency ratios of 1.05 and 1.1, the effect of stiffness becomes more prominent.

The energy values are higher in the regions where the dominant effect more effectively contributes to the resonance condition, indicating that whichever parameter—mass or stiffness—is better tuned to the excitation frequency, it facilitates greater energy accumulation in the system.

5. DISCUSSION

Throughout this study, it has been demonstrated that the number of attachments, their spatial configuration, the harmonic excitation frequency, the damping ratio, and the frequency ratio exert substantial influences on the amount of harvested energy.

The first six natural frequencies of the plate examined in the present study have been observed to decrease as discrete attachments have been added to the structure. This finding is consistent with the results reported by Cho et al. (2017) where it has been demonstrated that an increase in the number of attachments leads to a reduction in natural frequencies due to the increased inertia introduced by the added masses.

When the frequencies of the attachments are tuned to match the first mode of the plate, the total collected energy has been observed to increase with the number of attachments. However, this increase does not translate proportionally to each individual attachment, as a noticeable reduction in energy per attachment occurs. This reduction becomes less pronounced in configurations that are not frequency-matched. Such behavior can be explained by the broader resonance behavior of the coupled system, which becomes more distributed as the number of attachments increases. A similar trend has been reported by Koç et al. (2005) who have shown that increasing the number of energy sinks improves overall energy absorption, but with diminishing returns after a certain count. Their findings support the idea that, although a greater number of oscillators or attachments enhances total damping performance, the benefit gained from each additional unit decreases as modal coupling saturates. These results highlight the importance of balancing attachment number and frequency alignment when designing efficient energy-capturing systems.

An increase in the collected energy has been observed when the attachments are placed closer to the center of the plate. This behavior can be attributed to the combination of fixed boundary conditions, the square geometry of the plate, and the harmonic excitation applied precisely at its center, all of which contribute to the formation of maximum displacement—and consequently maximum kinetic energy—in the central region. A similar observation has been reported by Cho et al. (2017) where it has been

shown that attachment placement plays a critical role in the system's dynamic behavior, particularly when positioned near regions of high modal displacement. Their findings have emphasized that such locations amplify the attachments' influence on vibrational modes and frequency shifts. The consistency between the present results and the findings of Cho et al. (2017) reinforces the significance of strategic attachment positioning for maximizing energy transfer and control effectiveness.

As the damping ratio increases, the system's ability to retain vibrational energy has been observed to decrease, resulting in a noticeable reduction in the amount of energy collected. This finding underscores the critical role of damping in energy harvesting systems, where excessive damping may suppress vibrational response to the extent that it limits usable energy extraction. A similar observation has been made by Gavic (2006) who has numerically investigated the effect of damping in a beam–plate coupled system. In that study, damping has been found to significantly influence the total energy dissipation within the structure, although it has had a limited effect on the energy distribution between the connected components. Taken together, these results highlight that while damping is essential for controlling excessive vibration, its optimization is equally important to avoid compromising energy transfer and harvesting performance.

Considering the frequency ratio, the highest amount of harvested energy was obtained when the attachments were coupled with the first mode of the plate and the harmonic excitation frequency matched the plate's first mode frequency. Based on the frequency equation, it was observed that both the mass and stiffness of the attachments play significant roles: the mass effect becomes more dominant when the frequency ratio is below 1, while the stiffness effect becomes more dominant when the frequency ratio exceeds 1.

6. CONCLUSION

During this thesis study, the effects of various constructive parameters – such as the number of attachments individually placed on the main structural element (the plate), their locations, the damping ratio, and the frequency ratio – on the maximum amount of energy that can be harvested when the plate is subjected to harmonic excitation were investigated.

In the following paragraphs, the results are summarized in bullet points, and suggestions are provided regarding the aspects not addressed in this thesis as well as possible directions for future studies.

- The increase in the number of attachments leads to an enhancement in the total harvested energy; however, the energy harvested per attachment decreases.
- Placing the attachments closer to the center of the plate increases the energy harvesting efficiency.
- Maximum energy harvesting is achieved when frequency synchronization is established between the attachments and the plate (frequency ratio = 1).
- As the damping ratio increases, the energy that can be harvested by the system decreases.
- The attachment parameters (mass and spring constant) have a direct impact on the frequency ratio and play a crucial role in determining the energy harvesting efficiency.

Similarly, the following recommendations are provided below.

- The material effects could be evaluated by applying similar models to different material types (e.g., composite plates).
- In addition to harmonic excitation, the system's energy harvesting performance could be investigated under random excitations.
- Similar analyses could be performed on plates with different boundary conditions.
- By incorporating magnetic or piezoelectric-based active damping mechanisms instead of structural damping, energy harvesting efficiency could be improved.

REFERENCES

Ahmed, R., Atiyah, K., & Abdulsahib, I. (2020). Control of vibration by using dynamic vibration absorber. *IOP Conference Series: Materials Science and Engineering.* Purpose-Led-Publishing. doi:10.1088/1757-899X/881/1/012080

Ali, S., & Adhikari, S. (2013, July). Energy Harvesting Dynamic Vibration Absorbers. *Journal of Applied Mechanics, 80*. doi:10.1115/1.4007967

Avalos, D., Larrondo, H., & Laura, P. (1993). *Vibrations of a simply supported plate carrying an elastically mounted concentrated mass.* Great Britain: Pergamon Press.

Cao, Y., Zhong, R., Shao, D., Wang, Q., & Guan, X. (2019). Dynamic Analysis of Rectangular Plate Stiffened by Any Number of Beams with Different Lengths and Orientations. *Shock and Vibration*. doi:https://doi.org/10.1155/2019/2364515

Chalasani, S., & Conrad, J. (2008). A Survey of Energy Harvesting Sources for Embedded Systems. *IEEE*, 442-447.

Chiba, M., & Sugimoto, T. (2003). Vibration characteristics of a cantilever plate with attached spring-mass system. *Journal of sound and vibration*, 237-263.

Cho, D., Kim, J.-H., Choi, T., Kim, B., & Vladimir, N. (2017). Free and forced vibration analysis of arbitrarily supported rectangular plate systems with attachments and openings. *Engineering Structures*. doi:https://doi.org/10.1016/j.engstruct.2017.12.032

Den Hartog, J. (1947). *Mechanical Vibrations.* New York and London: McGraw-Hill Book Company, Inc.

Erturk, A., & Inman, D. (2011). *Piezoelectric Energy Harvesting.* United Kingdom: John Wiley & Sons, Ltd.

Gürgöze, M. (1994). On the eigenfrequencies of a cantilever beam with attached tip mass and a spring-mass system. *Journal of Sound and Vibration*, 149-162.

Ingber, M., Pate, A., & Salazar, J. (1992). Vibration of a clamped plate with concentrated mass and spring attachments. *Journal of Sound and Vibration*, 143-166.

Katı, H., & Gökdağ, H. (2019). Multi-step differential transform method for free vibration analysis of beams with tip mass. *Journal of the Faculty of Engineering and Architecture of Gazi University*, 1679-1693. doi:10.17341/gazimmfd.571480

Koç, I., Carcaterra, A., Xu, Z., & Akay, A. (2005). Energy sinks: Vibration absorption by an optimal set of undamped oscillators. *The Journal of the Acoustical Society of America*, 3031-3042.

Kolvik, G. (2012). Higher order shear deformation plate theory [Master's thesis, University of Oslo]. Norwegian Open Research Archives.

Kopmaz, O., & Telli, S. (2002). Free vibrations of rectangular plate carrying a distributed mass. *Journal of Sound and Vibration*, 39-57. doi:10.1006/jsvi.2001.3977

Magrab, E. (2007). Natural frequencies and mode shapes of Timoshenko beams with attachments. *Journal of Vibration and Control*, 905-934. doi:10.1177/1077546307078828

Özgüven, E. (2024). Tuned vibration absorber design methodology for systems with cubic stiffness nonlinearity [Master's thesis, Middle East Technical University]

Pavic´, G. (2006). Numerical study of vibration damping, energy and energy flow in a beam-plate system. *Journal of Sound and Vibration*, 902-931. doi:doi:10.1016/j.jsv.2005.07.020

Posiadala, B. (1997, February). Free vibrations of uniform Timoshenko beams with attachments. *Journal of Sound and Vibration*, 359-369.

Ramu, I., & Mohanty, S. (2012). Study on Free Vibration Analysis of Rectangular Plate Using Finite Element Method. *Procedia Engineering*, 2758-2766. doi:10.1016/j.proeng.2012.06.323

Rana, R., & Soong, T. (1998). Parametric study and simplified design of tuned mass dampers. *Elsevier*, 193-204.

Rao, S. (2007). *Vibration of Continuous Systems.* Hoboken, New Jersey: Jonn Wiley & Sons, Inc.,.

Reddy, J. (2007). *Theory and Analysis of Elastic Plates and Shells.* Boca Raton: CRC Press.

Samani, F., Pellicano, F., & Masoumi, A. (2013). Performance of dynamic vibration absorbers for beams subjected to moving loads. *Springer*, 1065-1079. doi:10.1007/s11071-013-0853-4

Sezer, N., & Koç, M. (2021). A comprehensive review on the state-of-the-art of piezoelectric energy harvesting. *Nano Energy*. https://doi.org/10.1016/j.nanoen.2020.105567 adresinden alındı

Timoshenko, S., & WOINOWSKY-KRIEGER, S. (1989). *Theory of Plates and Shells.* New York: McGraw-Hıll Book Company.

Toprak, A., & Tigli, O. (2014). Piezoelectric energy harvesting: State-of-the-art and challenges. *Applied Physics*. doi:10.1063/1.4896166

Wagner, N., & Helfrich , R. (2017). *Dynamic Vibration Absorbers and its Applications.* Stuttgart: ResearchGate.

Wu, J.-S., & Chou, H.-M. (1998, June). Free vibration analysis of a cantilever beam carrying any number of elastically mounted point masses with the analytical-and-numerical-combined method. *Journal of Sound and Vibration*, 317-332.

Wu, J.-S., & Luo, S.-S. (1997). Use of the analytical-and-numerical-combined method in the free vibration analysis of rectangular plate with any number of point masses and translational springs. *Journal of Sound and Vibration*, 179-194.

Wu, J.-S., Chou, H.-M., & Chen, D.-W. (2003). Free vibration analysis of a rectangular plate carrying multiple various concentrated elements. *J. Multi-body Dynamics*, 171-183.

Yıldız, A., & Kopmaz, O. (2017). Experimental and computational validation of an analytical model of free vibration of a rectangular plate carrying a distributed mass. *International Journal of Advances in Engineering & Technology*, 233-242.

Yu, S. (2009). Free and forced flexural vibration analysis of cantilever plates. *Journal of Sound and Vibration*, 270-285.

Zheng, H., Mao, X.-Y., Ding, H., & Chen, L. (2024). Distributed control of a plate platform by NES-cells. *Mechanical Systems and Signal Processing*. doi:https://doi.org/10.1016/j.ymssp.2024.111128

Zhou, D., & Ji, T. (2012). Free vibration of rectangular plates with attached discrete sprung masses. *Shock and Vibration*, 101-118. doi:10.3233/SAV-2012-0618

CURRICULUM VITAE

Surname, Name : MANTAR, Serkan

Foreign Languages : English

Education

Degree	Institute	Graduation Date
Master	Aydin Adnan Menderes University, Graduate School of Natural and Applied Sciences, Mechanical Engineering	Ongoing
Bachelor	Sakarya University, Faculty of Engineering, Mechanical Engineering	2017

WORK EXPERIENCE

Year	Place/Institution	Title
2025-	Marmara University, Mechanical Engineering Department	Research Assistant
2021-2022	OKT Trailer	Education of Engineering Formation

ACADEMIC PUBLICATIONS

1. PROCEEDINGS

S. MANTAR and T. ERAY, “Investigation of The Effect of Structural Parameters of Attachments On The Plate On Energy Harvesting,” presented at the 5th International Congress of Engineering and Natural Sciences , 2025.